Applied Geochemistry 155 (2023) 105705

Contents lists available at ScienceDirect

Applied Geochemistry

journal homepage: www.elsevier.com/locate/apgeochem

The natural magnesite efficacy on arsenic extraction from water and alkaline influence on metal release in water

Regina Irunde [a,b,c,*], Fanuel J. Ligate [a,b,e], Julian Ijumulana [a,b,d], Arslan Ahmad [a,g], Jyoti Prakash Maity [f], Rajabu Hamisi [a], Joseph Y.N. Philip [c], Kessy Fidel Kilulya [c], Erik Karltun [h], Joseph Mtamba [b], Prosun Bhattacharya [a], Felix Mtalo [b]

[a] KTH-International Groundwater Arsenic Research Group, Department of Sustainable Development, Environmental Science and Engineering, KTH Royal Institute of Technology, Teknikringen 10B, SE-100 44, Stockholm, Sweden
[b] Department of Water Resources Engineering, College of Engineering and Technology, University of Dar es Salaam, Dar es Salaam, Tanzania
[c] Chemistry Department, College of Natural and Applied Sciences, University of Dar es Salaam, Tanzania
[d] Department of Transportation and Geotechnical Engineering, College of Engineering and Technology, University of Dar es Salaam, Dar es Salaam, Tanzania
[e] Department of Chemistry, Mkwawa College of Education, University of Dar es Salaam, Tanzania
[f] Environmental Science Laboratory, Department of Chemistry, School of Applied Sciences, KIIT Deemed to be University, Bhubaneswar, Odisha, 751024, India
[g] SIBELCO Ankerpoort NV, Op de Bos 300, 6223, EP, Maastricht, the Netherlands
[h] Department of Soil and Environment, Swedish University of Agricultural Sciences, SLU, P.O. Box 7014, SE-750 07, Uppsala, Sweden

ARTICLE INFO

Editorial handling by: Prof. M. Kersten

Keywords:
Arsenic removal
Calcined magnesite
Contact time and pH
Kinetics and isotherm
Natural water

ABSTRACT

Arsenic (As) removal studies were carried out through batch experiments to investigate the performance of the locally available calcined magnesite mineral rocks from Tanzania. Natural water from a stream source in Tanzania and the prepared synthetic water at the laboratory were used for the studies. Parameters such as initial As concentration, calcined magnesite dosage, contact time and pH were evaluated for As removal using an overhead rea×2 shaker. Arsenic concentration was reduced from 5.3 to 1.1 mg/L As(V) at 180 min when 0.5 g/L calcined magnesite was applied to a synthetic water sample, whereas the concentration of 117 μg/L As(V) and 5.2 μg/L As(III) was reduced to below 0.1 μg/L in natural water. An increase in calcined magnesite dosage resulted in increased As removal up to below 0.01 mg/L. The calcined magnesite raised the pH of the water sample from 6.8 to 10 when the applied dosage increased between 0.002 g/L and 0.05 g/L. The pH was constant at around 10 even when the amount of 0.05 g/L was added 2000 times. Despite the high pH, the amount of magnesium released in water was low. The calcination of magnesite at 500 °C increased surface area by 4 times as compared to the natural magnesite and X-ray diffraction showed presence of $MgCO_3$ phase as the dominant phase at this temperature. The reaction kinetics of As removal on 0.5 g/L calcined magnesite fitted with the pseudo-second-order ($R^2 = 0.96$). Reaction isotherm was strongly fitted with Freundlich isotherm ($R^2 = 0.98$). Linear regression and artificial intelligence neural network showed the As removal was influenced by both contact time and pH. Arsenic can be removed from As water using calcined magnesite and will be suitable for water treatment around gold mining areas.

1. Introduction

Arsenic (As) is a toxic element that occurs naturally in the earth's crust (Duker et al., 2005; Mandal and Suzuki, 2002). Arsenic contamination in drinking water sources has been a global challenge since 1990's when As was first detected from tube-well water in the northern district of Bangladesh (Flanagan et al., 2012). Its occurrence in the environment is due to weathering processes of rocks and sulfidic minerals (Bhattacharya et al.,1997, 2002, 2004, 2007; Mohan and Pittman, 2007). The oxidation of sulfidic minerals such as arsenopyrites, releases As into water sources (Islam et al., 2013). The As release in the environment can also be contributed by anthropogenic activities such as agriculture, mining, and industrial wastes (Finkelman, 2004; Mandal and Suzuki, 2002; Rukh et al., 2017). Environmental conditions such as

* Corresponding author. KTH-International Groundwater Arsenic Research Group, Department of Sustainable Development, Environmental Science and Engineering, KTH Royal Institute of Technology, Teknikringen 10B, SE-100 44, Stockholm, Sweden.
E-mail address: irunde@kth.se (R. Irunde).

https://doi.org/10.1016/j.apgeochem.2023.105705
Received 18 September 2022; Received in revised form 28 May 2023; Accepted 29 May 2023
Available online 3 June 2023

redox potential also influences the mobility of inorganic As species such as As(V) and As(III) (Violante et al., 2010). It is already known that As species distribution in the environment is controlled by redox potential (Eh) and pH in which As(V) species ($H_3AsO_4^0$, $H_2AsO_4^-$, $HAsO_4^{2-}$ or AsO_4^{3-}) dominate in the oxidizing environment and As(III), ($H_3AsO_3^0$; $H_2AsO_3^-$; $HAsO_3^{2-}$; AsO_3^{3-}) dominate in the reducing environment (Gupta and Chen, 1978). At pH below 2, the uncharged elemental As is dominant. Furthermore, the negatively charged arsenate that dominates at pH between 2 and 6 is $H_2AsO_4^-$ and $HAsO_4^{2-}$ between pH 6 and 8 while the negatively charged arsenite $HAsO_3^{2-}$ dominates at pH 9 or above (Gustafsson and Bhattacharya, 2007).

The presence of As concentrations exceeding 10 μg/L, the critical level given by the World Health Organization (WHO) in their drinking water guidelines (Cotruvo, 2017) has been reported around gold-mining areas in Tanzania (Almås and Manoko, 2012; Kassenga and Mato, 2008; Lucca, 2017; Nyanza et al., 2014; Taylor et al., 2005) and health effects among the population around gold mining area are already reported. The deleterious impact on human health include skin lesions such as hyperkeratosis and pigmentation changes, black-foot disease, circulatory disorders, diabetes, cancers of the bladder, lung, kidney, and liver (Gbaruko et al., 2008; Smith et al., 1992), respiratory disorders, nervous disorders, abdominal disorders, premature birth and low weight to born babies (Ahoulé et al., 2015; Jain and Ali, 2000; Mandal and Suzuki, 2002; Mohan and Pittman, 2007; Raj and Maiti, 2020). In this case, there is a need to investigate simple methods that remove As from water to secure society from excessive As exposure.

Removal of As from water is accomplished by several techniques such as precipitation-coprecipitation, coagulation from iron or alum, membrane filtration, surface-complexation, ion-exchange, reverse osmosis, electrodialysis, nanofiltration and adsorption (Ahmad et al., 2017, 2018; Litter et al., 2019; Maity et al., 2019, 2021; Wang et al., 2018). The adsorption method has been the most preferred technique especially in low-income countries because of cost effectiveness (Ayoob et al., 2007; Maji et al., 2008). Local available materials such as magnesite, contain Mg^{2+} ions with affinity for As at pH above 7 (Paikaray et al., 2018). Once As contaminated water is in contact with magnesite for long enough time, the As will be precipitated as $Mg_3(AsO_4)_2.4H_2O$ if pH is high (Wu et al., 2017). Precipitation, coprecipitation and/or sorption mechanisms of As(V) in $Mg(OH)_2$ under presence of carbonate has been hypothesized and reported to occur at higher pH above 11 (McNeill and Edwards, 1997). Removal of As from water using natural mineral rocks have been reported (Mishra et al., 2014). Natural mineral sorption materials are of interest due to their availability, efficiency, simple application and to some extent lower operational costs (Mishra et al., 2014). Locally available mineral rocks such as bauxite, magnesite, manganese ore, iron ore, and laterite are potentially useful for As removal since they provide high surface area, porosity, and stability (Mishra et al., 2014). Apart from As removal, magnesite is also applied in other purposes (Masindi, 2021) such as in the industry for building material and ceramics (Sadik et al., 2016). It is used for making inorganic fertilizers (Mulana and MustanirFuadi, 2019), to produce metallic magnesium and for removal of copper from water (Kıpçak and Isıyel, 2015), for phosphorus removal (Wei et al., 2019). The prominent magnesite deposits in Tanzania occur around Moshi region where the best grade of magnesite has been mined and exported as building material while the lower grade is left in the site as a waste. The lower grade is easily available and useful material for As removal from water sources. The current study aims to evaluate the efficiency of the locally available calcined magnesite on As removal from water sources and release of trace metals due to alkaline condition after water treatment. The study is limited to not control pH with chemicals when it raises because calcined magnesite will be applied by the local society for arsenic removal from water sources around gold mining areas in northern region of Geita and Mara Tanzania and hence next step to lower pH after water treatment is recommended.

Arsenic removal using magnesite dosage of 10 g/L magnesite is reported in South Africa (Masindi and Gitari, 2016) where the equilibrium time was reported reached at 15 minutes (min). However, the current information about application of natural deposited magnesite as well as calcined magnesite for arsenic removal from drinking water sources is very limited. In the current study, the efficiency of the calcined magnesite is evaluated on As removal from drinking water sample. Furthermore, the release of trace metals from the calcined magnesite material into the treated water sample was studied. The minimum calcined magnesite dosage between 50 g/L, 5 g/L 0.5 g/L and 0.05 g/L that is capable to remove As was investigated since the previous reported dosage by Masindi and Gitari (2016) was a high dosage in 1 L of the water sample. To the best of our knowledge, the current study is the first evaluation study on application of locally available calcined magnesite from Tanzania for As removal from drinking water sources. The evaluation of As removal using calcined magnesite was carried at a laboratory scale through batch experiments using natural drinking water sample whereas for the high As concentration removal, synthetic As(V) water sample was used.

2. Materials and methods

2.1. Materials

Natural magnesite rock minerals were collected from a bulk deposit of magnesite in Chambogho in Same district, Moshi, Tanzania. Magnesite mineral rocks were brushed clean, washed, dried, crushed, ground, sieved to below 0.3 mm, calcined at 500 °C and thereafter used for As removal experiments. The natural water sample fetched from Masinki at latitude −1.48672°, longitude 34.50887°, elevation 1198 m in Tarime, Mara, Tanzania was used for As speciation and removal evaluation. Samples of water with different As concentrations were prepared in the laboratory to investigate the removal capacity of calcined magnesite at higher As concentrations.

2.2. Characterization of magnesite

A portion of raw and calcined magnesite powder sample was mounted on X-ray diffraction (XRD) sample-plate and introduced into the Panalytical Xpert Pro X-ray diffractometer (Cu–K-alpha1). The scan range (2θ) of diffractometer was 10–80° within 15 min (40 mA, 45 kV). The obtained XRD diffraction data were analyzed in X'Pert High-Score plus software under the database from International Center for diffraction data (ICDP PDF-4+ 2022) to identify mineral phases that exist in the magnesite sample. A portion of powder sample was introduced in JEOL field emission scanning electron microscope (FE-SEM-EDS, JSM-7000F) to determine elemental composition and the morphology of the material. Furthermore, the surface area of the material was analyzed using the Brunauer Emmett Teller (BET) method under adsorptive nitrogen (N_2) and equilibration interval of 15 s.

The content of iron (Fe) and As in the raw magnesite powder was investigated by digesting 5 g magnesite in 10 mL concentrated nitric acid, heated at 115 °C for 2 h. The filtrate was diluted with distilled water to 100 mL and measured at inductively coupled plasma atomic emission spectroscopy (ICP-OES, iCAP 6000).

2.3. Reagents

All purchased chemicals and reagents were of analytical grade. Sodium arsenate heptahydrate ($Na_2HAsO_4.7H_2O$) was used for the preparation of 100 mg/L As(V) stock solution. Deionized water was used for preparation of diluted solutions.

2.4. Experimental part and water sample analysis

A batch experiment was carried out to evaluate the efficiency of the calcined magnesite on As removal. Calcined magnesite powder dosage ranging from 0.5 to 50 g/L was applied in As water samples and agitated vigorously at room temperature. The batch water samples were analyzed using ICP-OES for total As, Al, Fe, Mg, Ca. An As speciation analysis was done using high performance liquid chromatography inductively coupled mass spectrometer (HPLC-ICP-MS) at ALS under method OV-19d with lower detection limit of 0.1 μg/L.

The quality check from sampling to instrumental analysis was considered to minimize error from measurements. Analytical instruments such as ICP-OES, were calibrated using analytical grade multi-standard solutions and the calibration model fit was recorded at $R^2 = 0.99$. For ICP-OES, the standard solution run was repeated after 8 samples to correct the instrument drift. The average of triplicate measurements was reported and the relative standard deviation was less than ±5%.

2.4.1. Natural water

The natural water sample from Masinki stream was analyzed using ICP-OES (iCAP 6000) and ion chromatography (IC, Dionex Dx-120) for the water quality parameters. The cations and anions present were simulated using Visual MINTEQ (https://vminteq.lwr.kth.se/download/) to check the removal trend and saturation indexes.

Arsenic speciation was carried out in the laboratory at ALS Scandinavia in Sweden. The samples sent to ALS also included treated samples, 100 g calcined magnesite per L, to check how magnesite removes As ions from Tanzanian natural water. The samples were analyzed using HPLC-ICP-MS to determine the levels of inorganic As species (As(V), As(III)) and organic species. The values of As (III) and As(V) were inserted in visual MINTEQ to investigate removal trend of As against increase in the adsorbent dosage and saturation indexes.

2.4.2. Preparation of synthetic As sample solution

Arsenic solutions were prepared through dilution of the stock As solution of 100 mg/L $Na_2HAsO_4.7H_2O$. The initial As concentrations prepared at near neutral pH varied from 0.1, 0.5, 1, 2, 3, 5 and 10 mg/L for evaluating arsenic removal with influence of contact time, initial concentrations, dosage and pH. In the As(V) solution, 0.5 g/L, 5 g/L, and 50 g/L calcined magnesite was introduced and agitated vigorously at 70 revolutions per minute (rpm) at different times such as 2 min, 5 min, 15 min up to 4 hours (h). Samples were filtered using 0.45 μm filter and kept in the fridge at 4 °C for the subsequent analyses. The samples with pH higher than 10 and above were acidified using 2 drops of 20% nitric acid (HNO_3).

Extraction of As from calcined magnesite was evaluated using 10 mL of 0.1 M NaOH introduced in 1g of spent material and shaked vigorously for 2 h.

2.4.3. Adsorbent dosage

An efficient minimum calcined magnesite dosage for enhancing removal in this study was checked between 0.5 g/L, and 5 g/L and 50 g/L. To determine the best calcined magnesite dosage, the amount in concentration was varied from 0.05 g/L, 0.5 g/L, 5 g/L, 50 g/L, and 100 g/L and shaked with As solution at near neutral initial pHs. Preliminary pH tests in this study involved 200 g/L calcined magnesite at initial pH 1.51 since pH 4.2 and 2.3 raised pH above 10.

The relationship of parameters such as concentrations, contact time, dosage, pH, volume on influencing As removal from water sample was checked using linear regression as well as artificial neural network in SPSS software version 28, to evaluate how each parameter influences removal and which dosage provides less error in the treatment system.

3. Results

3.1. Characterization of calcined magnesite

The XRD analysis shows crystalline magnesium carbonate ($MgCO_3$) as the main phase in the locally available raw and calcined magnesite material from Chambogho, Tanzania. The other mineral phases in the magnesite powder were magnesium iron carbonate ($Mg_{0.99}$ $Fe_{0.01}(CO_3)$, iron carbonate ($Fe(CO)_3$), and silicon dioxide (SiO_2). In the calcined magnesite, the peaks for $MgCO_3$ were positioned at 32.8°,35.9°, 43°, 51.7° 54°, 61°, 62°, 68.5°, 70.5°, 76° and 77° (Fig. 1, Table S1b). The phase heterogeneity was also noticed when several phases appear in the same peak such as $MgCO_3$, $MgFe(CO)_3$, $FeCO_3$and Fe_2O_3 appeared together at positions 32.8°, 35.9°, 43°, 66° and 70.5°. A similar trend were noticed for the overlapping peaks for $MgCO_3$, $MgFe(CO)_3$, $FeCO_3$, Fe_2O_3, and MgO at position 43°; MgO and SiO_2 at position 21°; $MgCO_3$, $MgFe(CO)_3$ and $FeCO_3$ at position 51.7°; $MgFe(CO)_3$, $FeCO_3$ and Fe_2O_3 at position 66.5°; $MgFe(CO)_3$and $FeCO_3$ at position 38.9°, 46.9°, 69.4°; $MgCO_3$, $MgFe(CO)_3$, $FeCO_3$and MgO_2 at position 54° and $MgCO_3$, MgFe $(CO)_3$, $FeCO_3$ and MgO at positions 61° and 62° respectively.

The calcination of magnesite at temperature of 500 °C (Xu et al., 2010) formed less MgO to be ranked in Xpert high score software and the main phase ranked after calcination was $MgCO_3$ (Fig. 1, Figs. S1a and b, Tables S1a and b) however under phase restriction, the MgO was recorded at position 21°, 43° and 62°. It was reported that calcined magnesite can yield high MgO at higher temperatures from 1000 °C (Masindi, 2021) even though 600, 700 and 800 °C are also reported to yield MgO (Salameh et al., 2015). The previously reported temperature of 350 °C converts iron carbonate ($FeCO_3$) to hematite while 600 °C for 2 h was enough to convert all siderite to iron oxide (Zhao et al., 2014). The MgO pure powder was reported to raise pH of the solution up to 13–14 (Natsi et al., 2023) which was noted in this study.

The presence of As in the calcined magnesite was recorded when digested magnesite sample analyzed in ICP-OES had traces of As of about 0.004 mg/L. However, it was not easier to observe new crystalline phases in XRD after As treatment, but under restriction, very small phase of magnesium arsenate were observed.

The field emission FE-SEM-EDS revealed that the surface morphology of calcined magnesite was heterogeneous due to the presence of different chemical elements (Fig. 2). The heterogeneous surface of calcined magnesite provides active site for As removal. Spectrum 2 in Figure 2 shows the presence of carbon (C), oxygen (O), magnesium (Mg), silica (Si), calcium (Ca) and iron (Fe) with atomic percentage of 13.8%, 63%, 20%, 0.6%, 0.2%, and 0.3% respectively. The presence of C, O, Mg, Ca and heterogeneous surfaces was also reported by Masindi and Gitari, 2016). Furthermore, ICP-OES confirmed the presence of Fe in the digested raw magnesite with concentrations of about 87.48 mg/L, which is also useful for removal of As.

BET surface area analysis shows higher surface area in calcined magnesite 18.07 m^2/g than in raw magnesite 5.13 m^2/g. The surface area is important factor for the effective removal of As from water. Pore size and volume also affect process of As removal, as revealed by the observed reduction in pore size diameter from 8.99 nm to 8.68 nm. The

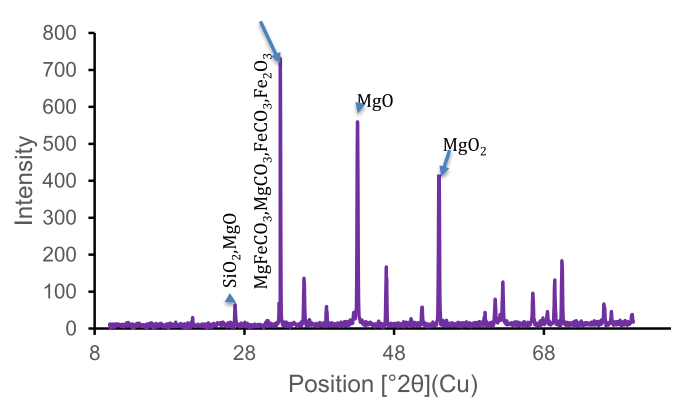

Fig. 1. XRD spectrum of magnesite shows the main phase of calcined magnesite.

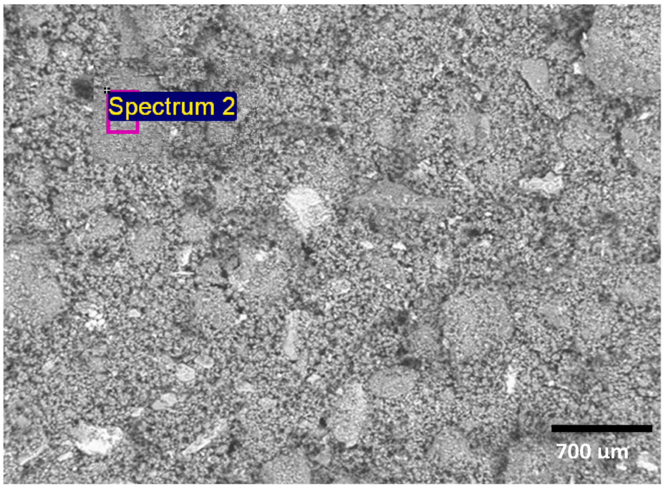

Fig. 2. SEM picture showing heterogeneous surface of calcined magnesite.

porous nature of the material is also believed to increase the removal efficiency during the pore filling process.

3.2. Batch experiment for arsenic removal

The As water samples were poured in containers and agitated vigorously using an overhead-rex2 shaker. Both natural drinking water and synthetic water was used for evaluation of As removal on calcined magnesite. It takes a short time to reach high removal efficiency when using overhead-rex2 shaker. The calcined magnesite was observed to absorb water to about 40% which reduces amount of water sample during the batch experiment. The previous study TGA data from the previous studies (Liang et al., 2022; Natsi et al., 2023) indicated that magnesite loses water with an increase in temperature (Figs. S2 and S3).

3.2.1. Natural drinking water sample

The natural water sample exhibited high concentration of anions such as sulphate (SO_4^{2-}) 479 mg/L which is above WHO limit of 250 mg/L (Cotruvo, 2017), followed by nitrate (NO_3^-) 59.5 mg/L, chloride (Cl^-) 18. 2 mg/L, fluoride (F^-) 2.3 mg/L and phosphate (PO_4^{3-}) 1.3 mg/L. The sample was characterised by high total concentrations of calcium (Ca^{2+}), magnesium (Mg^{2+}) and nickel (Ni^{2+}) 45 mg/L, 16.37 mg/L and 6.09 mg/L respectively. The concentration of other cations such as Cd^{2+}, Co^{2+}, Cu^{2+}, Fe^{2+}, Mn^{2+}, Mo(VI), Pb^{2+}, Sr^{2+} Sb(III), Se(VI), Ti(OH)4, TL^{+1}, V(IV) and Li^{+1} (Note: the elements are represented as ions for the purpose of selecting specific ion in the Visual MINTEQ) were low. The presence of high calcium and sulphate rendered the water as of calcium-sulphate type. These species (anions and cations) including As species were simulated on visual MINTEQ version 3.1 to evaluate removal trends of As upon increase in dosage and determination saturation indices. The dosage amounts used in the visual MINTEQ was 0.001, 0.005, 0.008, 0.01. 0.03, 0.09, 5, 10, 20, 30 g/L which shows increase in As removal as the dosage increase (Table S3, Fig. S4). The removal of As (V) increased from 3.3% for an added amount of 0.001 g/L to 99.9% at 0.03 g/L while at 0.01 g/L removal was still 40% (Table S3). Furthermore, the element removed were influenced by pH simulated when 5 g/L $MgCO_3$ added in the solution shows stability of certain elements in a wide range of pH and reduction of removal as pH increases to 10 (Table S5). The removal trend acquired from visual MINTEQ was applied as a guide for As removal using calcined magnesite and similar removal trend as magnesite dosage increased was observed in section 3.2.2.

3.2.1.1. Saturation index simulation on visual MINTEQ as function of pH. The simulation of natural water in visual MINTEQ with the addition of 5 g/L $MgCO_3$ revealed a decrease in ionic strength from 0.41, 0.40 0.39, 0.39, 0.38, 0.27, 0.20, and increase in pH from 4, 6, 6.8, 7, 7.5, 10, and 12 respectively. However, at pH 13, the ionic strength raises to 0.27 with charge difference of 15.99%. The ionic strength affects the increase or decrease of ion activity in the solution. The higher the ionic strength, the lower the pH, in which enhances undersaturation of the mineral phases.

The mineral phases formation behavior in the solution of natural water dependst on the type of the mineral as pH increases from pH 4 to pH 13 (Table S4). The undersaturation of mineral phases was observed at lower pH 4 while some mineral was slightly oversaturated at the neutral pH 6.8 and oversaturation increases to pH 10 before it declined (Table S4). For pH 6.8, Some minerals were stable oversaturated in a wide range of pH from 6.8 to 13 while some mineral dissolved after pH 10. At pH 6.8, recorded minerals were magnesite, dolomite disordered, dolomite ordered, huntite, $NiCO_3$ with oversaturation indexes of 1.12, 1.56, 2.11, 2.30, and 0.53 respectively. Mineral phases that existed at pH 10 to mention few were aregonite, brucite, calcite, hydromagnesite, magnesite, $MgCO_3.5H_2O$, Nesquehonite, $Ni(OH)_2$ c, strontianite, and vaterite with oversaturation indexes of 1.86, 1.36, 1.99, 10.27, 3.23, 0.29, 0.42, 2.10, 0.85 and 1.43 respectively. Thus, the mineral phases observed at pH 10 and above have contributed on arsenic removal from water.

3.2.1.2. As speciation on natural water sample. Arsenic speciation of the natural water sample from Tanzania (Masinki stream) shows 117 μg/L As(V), 5.32 μg/L As(III), <0.2 μg/L monomethyl arsenate (MMA) and 0.83 μg/L dimethyl arsenate (DMA). The As(V) value was above WHO guideline for drinking water (Cotruvo, 2017). In the treatment of natural water with the calcined magnesite for 2 h, the As(III) and As(V) were reduced to <0.1 μg/L which is 99% As(V) removal, 98% As(III) while MMA was <0.2 μg/L and DMA was 0.36 μg/L. The observation shows that the removal of organically bound As on the calcined magnesite was less favorable compared to inorganic As species. On the other hand, As speciation in visual MINTEQ was found to be influenced by pH (Table S6). Thus, the dominance of arsenate [As(V)] and arsenite [As (III)] varies with an increase in pH.

3.2.2. Arsenic removal from synthetic arsenic solution

This section evaluates removal using prepared solution from the laboratory for higher As concentrations than the levels of As present in natural water in Tanzania. Four calcined magnesite dosage 0.05, 0.5, 5, 50 g/L were evaluated to provide a more efficient treatment system with less error.

3.2.2.1. Concentration dependent removal. The removal percentage of As on 0.5 g/L calcined magnesite decreased as initial concentrations of As increases from 1 mg/L to 20 mg/L that is comparable to the previous reported results (Masindi et al., 2014). The initial As concentration of 1 mg/L on 0.5 g/L calcined magnesite that was agitated for 30 min on overhead reax2 shaker showed high As removal of 63% (Table S7). For the highest initial 20 mg/L As, only 26% As removal was achieved on 0.5 g/L of calcined magnesite (Fig. 3). In comparison with higher dosages of 5 g/L and 50 g/L, the As removal was recorded increasing up to 99% with an corresponding increase in initial As concentration (Fig. S8).

Observations showed more contact time is required to allow As removal on 0.5 g/L calcined magnesite for 5.3 mg/L As since only 79.6% As removal was reached after 3 h. In general, the As removal percentage observed in this study was increasing with increased dosage of calcined magnesite similar to the removal observed through the visual MINTEQ simulations. Thus, observation at equilibrium time for 0.5 g/L calcined magnesite was slow, as at 30 min achieved removal of 37% while 5 g/L shortened equilibrium time (at 5 min) gave 93%. Hence the equilibrium time is achieved fast at a higher dosage of about 5 g/L than the lower dosage.

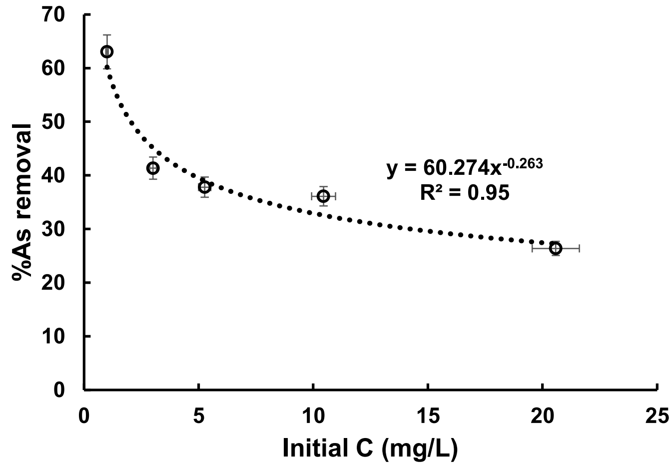

Fig. 3. Arsenic removal with initial concentrations at 30 min, 0.5 g/L calcined magnesite.

3.2.2.2. Effect of the dosage on pH and calcined magnesite release in water after treatment. The dosage of calcined magnesite was observed to raise pH abruptly when the water had an initial pH below 4. The rapid reaction between calcined magnesite and acidic solution raises pH up to 10 due to the presence of $MgCO_3$ and MgO which hydrolyses to form Mg $(OH)_2$ and HCO_3^- in the solution. The pH change also depends on the volume of the water sample, initial pH and dosage of calcined magnesite. The acidic water sample with pH 4 raises pH to 10 when 100 g of calcined magnesite was introduced per liter of water and agitated for 20 min, but the same amount of calcined magnesite dosage to water with an initial neutral pH 7 raised to about pH 9. At lower dosages, for example, 0.002 g/L of calcined magnesite added at initial pH 6.8 could not raise much pH (Fig. 4) when agitated for 15 min. The increase in pH was correlated to the amount of added calcined magnesite into the water sample that resulted to an increase of R^2 to 0.96 (Fig. S6). The equilibrium pH of 12 as a function of magnesite dosage was predicted from linear equation in Fig. S6 (Fig. 5).

The main mechanism of As removal at pH 10 can be a precipitation as represented by Equation (1). The Mg^{2+} ion from magnesite or Mg $(OH)_2$ reacts with AsO_4^{3-} at alkaline conditions to form an As precipitate of magnesium arsenate.

$$Mg^{2+}(aq) + AsO_4^{3-}(aq) \rightarrow Mg_3(AsO_4)_2(s) \quad (1)$$

The maximum removal was favored at higher pH which indicated formation of As precipitate.

There was no observed leaching of magnesium (Mg) from the calcined magnesite into water above WHO guideline even at higher pH 10. The elements dissolved in water after treatment such as Al. Fe. Mg

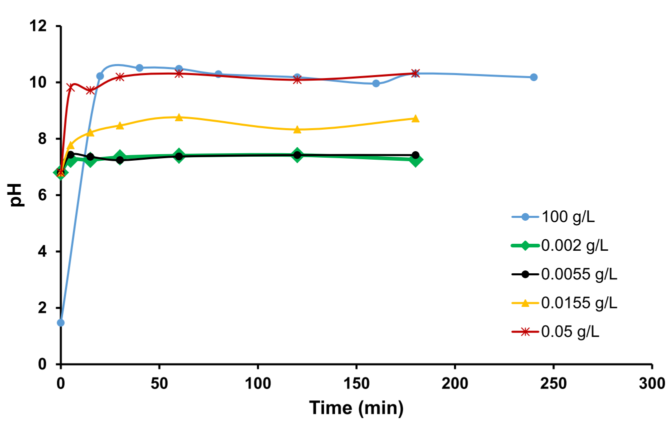

Fig. 4. Calcined magnesite behaviour of raising pH at different dosages.

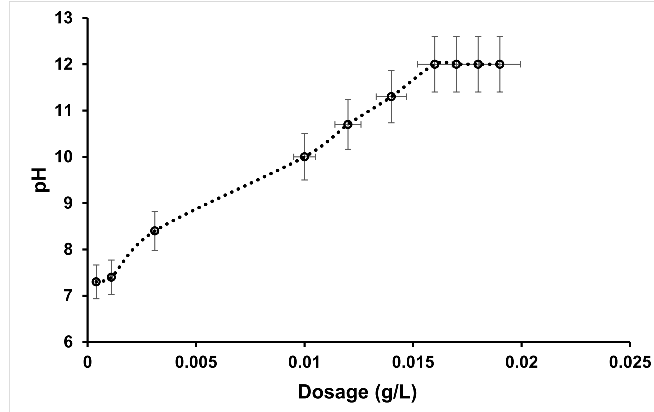

Fig. 5. Increase in pH as a function of dosage.

and Ca (Table 1) were analyzed to evaluate trace metals released in water during treatment. The treated water had pH value of 10 in which magnesium and calcium were less released and was below WHO guideline due to its tendency to form precipitate with As. The nature of aluminium did not tolerate pH 10, hence it was released in water with concentrations similar or slightly above the recommended guideline value of WHO. Furthermore, iron was not significant released in water due to its high affinity towards As species.

3.2.2.3. Removal capacity. Table 2 shows removal capacity (qt) at any time (t) as calcined magnesite dosage was used in descending order between 50 g/L to 0.05 g/L, where removal capacity inversely increased with time at low calcined magnesite dosage. Thus, removal capacity was ranging between 2.06 and 8.39 mg/g when small amount of material of 0.5 g/L was used. Other literature sources on natural minerals reported similar results such as manganese, 2.15 mg/g (Mohapatra et al., 2006), natural iron ore 0.4 mg/g (Zhang et al., 2004), modified calcined bauxite 1.57 mg/g (Bhakat et al., 2006); gibbsite 4.6 mg/g goethite 12.4 mg/g, oxisol 3.2 mg/g (Ladeira and Ciminelli, 2004) and siderite 1.04 mg/g (Guo et al., 2007).

The removal capacity (Equation S13) of calcined magnesite using dosage of 0.05 g/L, 0.5 g/L, 5 g/L, and 50 g/L, shows good trend for As removal since removal capacity increases with decrease in calcined magnesite dosage (Table 2). Also, the removal capacity increases with increase in contact time (Table 2) and 0.5 g/L fitted intraparticle diffusion (Equation S1) with R^2 of 0.89. Furthermore, the removal capacity was observed to increase with initial concentration with R^2 of 1 when 50 g/L of calcined magnesite was introduced in initial As concentrations ranging 0.1 mg/L to 30 mg/L (Fig. 5). The amount of 50 g/L calcined magnesite was a very high dosage to be added in which removes As up to 99% despite the concentration increase to 30 mg/L hence the interest was to investigate the minimum efficient dosage of calcined magnesite which we recommend 0.5 g/L. The lowest concentration of 0.1 mg/L removed using 50 g/L calcined magnesite showed 0.002 mg/g adsorption capacity while 5, 10, 20 and 30 mg/L showed removal capacity of 0.105 mg/g, 0.21 mg/g, 0.41 mg/and 0.61 mg/g, respectively. The current removal capacity are closer to the ones

Table 1
Average levels of elements released in water after treatment.

Elements released in water (mg/L)	Calcined magnesite dosage (g/L)					WHO (2017) (mg/L)
	100	50	5	0.5	0.05	
Aluminium (Al)	-0.135	0.005	0.19	0.10	0.33	0.2
Iron (Fe)	0.001	-	0.0003	0.002	0.002	0.3
Magnesium (Mg)	14.8	14.65	14.78	10.65	2.76	100
Calcium (Ca)	4.16	4.55	0.89	0.45	1.34	100

Table 2
Removal capacity from different magnesite dosage.

Dosage (g/L)	Initial As (mg/L)	qt (mg/g)	Contact time (min)
50	5.266	0.105	30–240
5	5.266	0.7–1.05	2–30
0.5	5.266	2.06–8.39	5–180
0.05	5.266	0.006	5–180

reported from natural iron oxides (Aredes et al., 2013). Previous study reported that 10 g/L of magnesite removes up to 20 mg/L in water sample (Masindi and Gitari, 2016), however, our study predicts that more than 30 mg/L can be removed on 5 g/L.

The removal capacity increases with increase in initial concentrations, because calcined magnesite provides enough surface area to accommodate more As removal on its active sites. The ability of calcined magnesite to remove As reveals presence of high affinity polyvalent elements towards As such as iron (Fe) (Equation (2)) which supported magnesite to have high efficiency. The iron oxide (Fe_2O_3) transformed from iron carbonate ($FeCO_3$) at 600 °C is reported to enhance As removal of about 10 mg/g (Zhao et al., 2014).

$$Fe^{3+}(aq) + AsO_4^{3-}(aq) \rightarrow Fe(AsO_4)(s) \quad (2)$$

The presence of iron in the magnesite was confirmed in the analysis of the digested raw magnesite hence it can attract arsenic due to its high affinity towards arsenic.

3.2.2.4. Chemical reactions for arsenic removal

3.2.2.4.1. Half-life of As solution. For determination of simple half-life, the first order of the rate law kinetics (Equation S7, Figure S7) was calculated from the calcined magnesite dosage of 0.05 g/L, 0.5 g/L, 5 g/L and 50 g/L (Table S10). Kinetic first-order rate law was fitted with R^2 of 0.93 for 0.5 g/L when 5.3 mg/L As was removed. The higher the dosage the faster the rate of reaction. The half-life for As was calculated and obtained as 2310, 87.7, 2, 0.3 min with respect to dosage 0.05 g/L 0.5 g/L, 5 g/L, 50 g/L (Table S10).

3.2.2.4.2. Equilibration reaction time. The equilibration time was observed around 5 min when 5 g/L calcined magnesite was introduced in 5.3 mg/L As sample. However, the prolonged equilibrium time beyond our hypothesized 30 min was observed when 0.5 g/L was applied in 5.3 mg/L As concentration. The equilibrium was fast at high dosage ranging 5 g/L to 50 g/L which removes As to about 99% within less than seconds. Masindi and Gitari (2016) also reported equilibrium time of 15 min when 10 g/L magnesite was used to remove 10 mg/L As. However, it was observed 0.5 g/L works better to remove 5.3 mg/L As sample than when 0.05 g/L was incorporated.

3.2.2.4.3. Pseudo second order for as reaction. Arsenic removal on calcined magnesite fitted well on pseudo-second-order kinetic (Equation S6) proposing chemical reaction as a controlling factor. For the high dosage of magnesite such as 50 g/L, pseudo second order was strongly fitted with R^2 of 1. The pseudo second order was significant even at calcined magnesite dosage of 0.5 g/L and 5 g/L. The correlation coefficient R^2 was observed to decrease as calcined magnesite dosage decreases from 50 g/L to 0.5 g/L as 1, 0.99 and 0.96, respectively. The minimum dosage of 0.5 g/L (Fig. 6) calcined magnesite was of interest to understand kinetic behavior of As reaction with calcined magnesite and its fit in pseudo second order gave equilibrium constant rate k_2 of 0.003 g min/mg. The chemical reactions in this section provide possible limiting factor of calcined magnesite on As removal, however to understand the reaction mechanism, further study on the application of the two dimensional infrared (IR) correlation spectroscopy (Li et al., 2021) is of relevance.

3.2.2.5. Isotherm reaction for As removal. The isotherm reaction for As removal following the Freundlich model (Fig. 7, Equation S9) indicates the presence of heterogenous sites energy (Chiban et al., 2011) in which

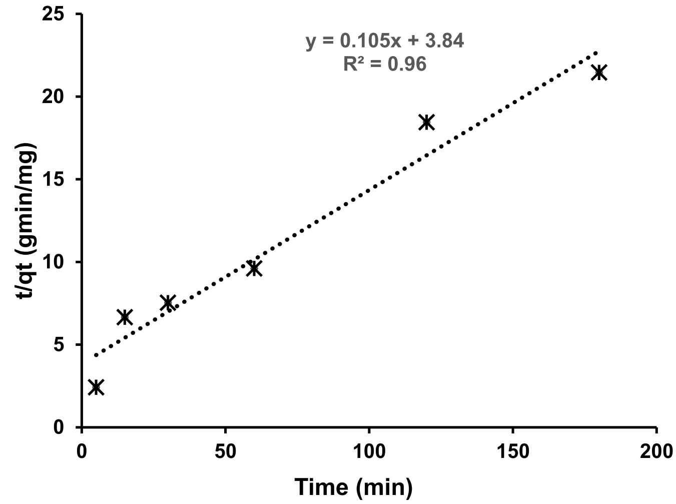

Fig. 6. Pseudo second order of 0.5 g/L calcined magnesite with R^2 of 0.96.

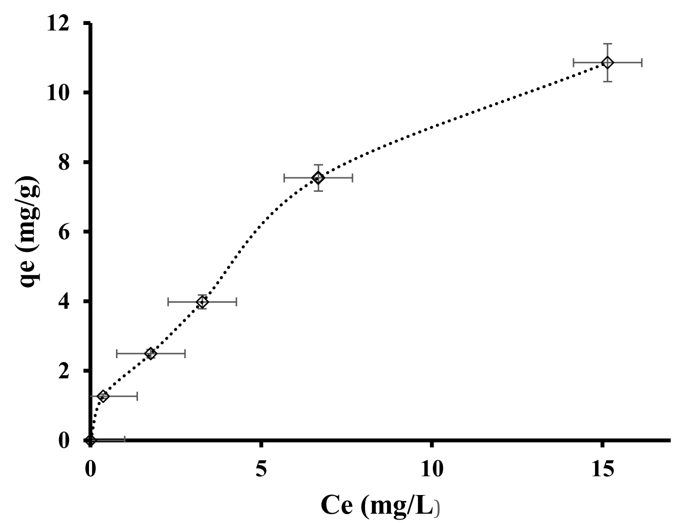

Fig. 7. Hysteresis loop for arsenic removal on 0.5 g/L calcined magnesite.

0.5 g/L calcined magnesite was sufficient to provide active sites for As removal in this study.

Chiban et al. (2011) stated that "reaction isotherms are mathematical models that describe the distribution of the contaminant among solid and liquid phases and are important data to understand the behavior of the removal". The hysteresis loop observed in Fig. 7 indicates the presence of mesoporous in the calcined magnesite (Xie et al., 2022) which enhances As removal during pore filling.

The initial concentrations ranging from 1–20 mg/L were agitated vigorously for 30 min. The result obtained fitted well with the Freundlich isotherm model (R^2 value of 0.98 (Fig. 8, Equation S9, Table S12) and n value of 1.54. The n value indicate favorable chemical reaction on As removal (Bakatula et al., 2017). From Fig. 8, k_f (equation S3) is 0.87 which can give Gibbs free energy $\Delta G°$ of 0.33 that means the removal process was non-spontaneous deviating from the process reported by Chiban et al., (2011). The calcined magnesite fitted Freundlich isotherm better even at higher dosage of 5 g/L and 50 g/L.

For the determination of the removal, the D-R isotherm model using equation S10, 11, and 12, the removal energy was 1290 kJ/mol which is greater than 16 kJ/mol (Bakatula et al., 2017) and hence the removal of As onto calcined magnesite can be controlled by the chemical reaction.

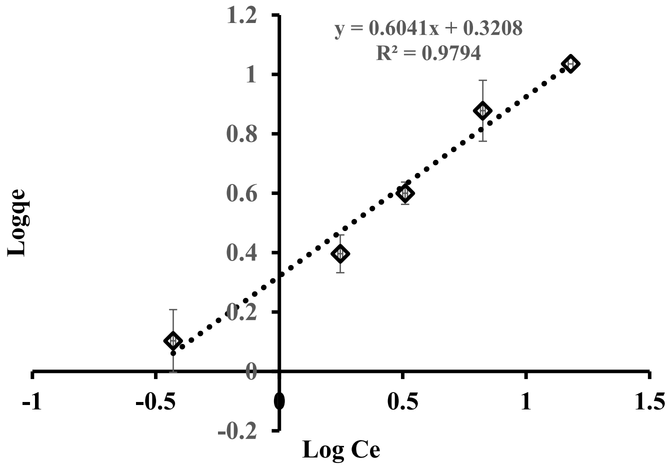

Fig. 8. Reaction removal isotherm fitted Freundlich isotherm with R^2 of 0.98 when 0.5 g/L calcined magnesite agitated for 30 min.

3.2.2.6. Statistics linear regression and artificial intelligence neural network for factors influencing as removal. Linear regression (Equation S2) assists to predict the best treatment system characterized with less error considering relationship between dependent and independent variables (Tables S13–S16). The linear regression analysis on SPSS version 28 revealed the significant model fit with F = 21.56, $R^2 = 0.92$, adjusted $R^2 = 0.87$, standard error = 0.5 when dosage of 0.5 g/L calcined magnesite was applied to remove As of 5.3 mg/L As in which concentration decreased depending on time and pH. The decrease in As concentration was much dependent on contact time since pH was not significant. The As concentration was strongly positive correlated to time and pH with r = 0.957.

$$\text{Conc} = -0.02\ \text{Time} - 0.25\ \text{pH} + 6.68 \tag{3}$$

The model was validated with a significant probability of 0.007 when predictors were time, and pH (Equation (3)). Thus, 91.5% of the model was linearly explained by time and pH. From this equation (3), an optimized values can be predicted to improve the water treatment system.

Similar experiment applying 0.05 g/L calcined magnesite revealed significant fit model with adjusted $R^2 = 0.93$, $R^2 = 0.95$, F = 38.31, error of 0.08 and a strong positive correlation of concentration to time, and pH with r = 0.98.

$$\text{Conc} = 0.001\ \text{Time} - 0.25\ \text{pH} + 6.91 \tag{4}$$

This equation model was significant at a probability value of 0.002 (Equation (4)). The removal dependent on pH since time was not significant.

In addition of 5 g/L, shows model significant F = 26.2 and probability of 0.01. The R^2 was recorded as 0.95, R^2 adjusted at 0.91, positive correlation (r) of 0.97 and error of 0.6. Removal of As depends on both time and pH since are significant (equation 5)

$$\text{Conc} = -0.17\ \text{Time} - 0.97\ \text{pH} + 11.74 \tag{5}$$

For 50 g/L calcined magnesite application, indicates significant model at probability <0.001 and F of 294.8. The relation coefficients are positive at r = 0.99, R^2 of 0.99 adjusted R^2 of 0.99 and error of 0.2. The removal was much influenced by pH since time was not significant.

$$\text{Conc} = -0.003\ \text{Time} - 1.14\ \text{pH} + 13.02 \tag{6}$$

In general, it was an interest to evaluate parameter mostly influences arsenic removal on the calcined magnesite and the linear regression shows dependence on contact time, and pH interchangeably according to the model error. The less model error was recorded by 0.05 g/L calcined magnesite followed by 50 g/L calcined magnesite. However, the highest best model to remove arsenic in a short time was 50 g/L calcined magnesite.

The knowledge of artificial neural network (Chakraborty et al., 2014) in SPSS version 28 can help to optimize experimental parameters and provide the strong relationship between removal parameters. It also highlights the most important parameter during removal process. The arsenic removal has strong relation with pH and contact time (Fig. S8, Fig. S9).

3.2.2.7. Extraction of arsenic from spent calcined magnesite. It was expected to release more As from this material at high pH, instead of that, the precipitate of calcined magnesite and As shows high stability at high pH. Thus, extraction of As using 0.1 NaOH was not successful. When 10 mL of 0.1 NaOH with pH 11.89 was poured in 50 g/L wet calcined magnesite spent on the removal of 10 mg/L As(V), agitated for 2 h, only 8% As was leached into the solution. For this observation of less release of As from calcined magnesite, then NaOH is not a good solution for desorption process from calcined magnesite. Also, low concentrations of Ca, Fe, Mg as (0.46, 0.02, 0.08) mg/L respectively which is below WHO guideline were released. Probably there was strong covalent bond formation which was in agreement with D-R isotherm model and the stabilization of As was enhanced.

4. Discussion and recommendations

The characterization of calcined magnesite at 500 ^oC (Xu et al., 2010) revealed presence of magnesium carbonate as a main phase, less MgO (recorded under phase restriction) as well as other phases which correlate to reported studies (Masindi, 2021; Masindi and Gitari, 2016). MgO presence was revealed when magnesite raised pH of the water sharply to 10 which is in agreement with previous reported pH (Natsi et al., 2023). The visual MINTEQ simulation on natural water in presence of 5 g/L $MgCO_3$ revealed oversaturation of mineral phases such as brucite, hydromagnesite, dolomite, calcite, magnesite, $MgCO_3.5H_2O$, nesquehonite which might influence As removal at high pH. Dissociation of magnesium carbonate (Equation S4, S5) (Shadrunova et al., 2022) and MgO in water sample forms $Mg(OH)_2$ (Tong and Tang, 1999) and other solubility products which raised pH to 10 creating alkaline environment for As precipitation as magnesium arsenate (McNeill and Edwards, 1997). It was reported that heating magnesite at 700 °C converts Mg, Fe, C into oxides which raise pH to form alkaline solution (Liang et al., 2022). Following alkaline condition, it was expected that arsenate which is lewis base (electron pair donor) could repel from magnesite surface and desorb into water, but As uptake was favored at this high pH creating more interest to investigate the phenomena. The presence of polyvalent metals such as iron, copper, titanium, zinc, manganese in the magnesite sample could have contributed to a synergic effect on As removal from water (Zhang et al., 2021).

The natural drinking water sample collected from Tarime - Tanzania, shows presence of As above WHO recommended limit of 0.01 mg/L (Cotruvo, 2017; Ligate et al., 2022). The presence of calcium sulphate water type was in agreement with the water type reported at Ethiopian great rift valley (Rango et al., 2013). The status of As around gold mining areas in Geita and Mara is expected to increase in future due to high As content analyzed to be present in rock samples collected around drinking water sources (Irunde et al., 2022) in which requires simple treatment to ensure the society is safe from contamination exposure. The health problem status linked to As contamination exposure is reported (Nyanza et al., 2019). Thus, application of locally available materials such as natural magnesite for As removal is of great importance.

Previous reports on locally available natural materials for As removal and their removal capacity are reviewed (Irunde et al., 2022). In the current study, removal capacity of the calcined magnesite was affected by pH, As initial concentration, calcined magnesite dosage and contact time. The higher dosage of calcined magnesite (50 g/L and 5 g/L) was observed to extract As in shorter contact time of 5 min and 20 min which can be correlated to the effect of 10 g/L reported in the earlier studies by Masindi and Gitari (2016). Thus, the low dosage of 0.5 g/L calcined magnesite exhibited increase in removal capacity from 2.06 mg/g to 8.39 mg/g as contact time increased from 5 to 180 min and also fitted intraparticle diffusion with R^2 0.89. The linear regression predicts the 0.05 g/L magnesite application as the less error model which should be applied for arsenic removal but during the experiment, not much uptake was revealed in this model hence the following less error model 50 g/L should be adopted during As removal since its efficiency was high at a short time due to higher magnesite dosage, and 99% of As removal was statistically influenced by contact time, and pH at probability <0.001. The strong relationship between As removal, pH and contact time was predicted by the application of artificial intelligence neural network (Figs. S8–9) in SPSS version 28. The artificial intelligence neural network predicts the pH as a high importance parameter to enhance As removal accompanied by contact time.

Removal process was observed to occur at higher pH 10 in which could cause release of metal into the water since pH influences the speciation of metals (Tahmasebpoor et al., 2022). The increase in As removal at high pH was also reported by Masindi et al. (2014) which related the effect of the high point of zero charge (pzc), pHpzc of around 11, that means, removal occurred because pH 10 was still below pHpzc of the calcined magnesite. The adjustment of pH is recommended after treatment before water supply to the community since WHO recommends pH 8.5 (Cotruvo, 2017). The adjustment of pH during application of calcined magnesite might be accomplished using activated carbon. Despite the higher pH, calcined magnesite did not release its constituent metals such as Mg, Ca, Fe above WHO except for Al, hence the adsorbent is useful for drinking water treatment purposes (Table 1).

Kinetic reaction fitted well with pseudo second order which correlates to other reported studies (Maji et al., 2008; Mohapatra et al., 2007; Sanou and Pare, 2021; Simsek and Beker, 2014). The pseudo second order assume chemical reaction to be a rate-limiting step involving valence forces through sharing electrons (Bulut and Tez, 2007). Furthermore, the isotherm fitted well on Freundlich model (Liu et al., 2014) which signify presence of active sites for As removal. The mesoporous structure of the magnesite material can be observed on the hyteresis curve (Fig. 7) which was similar reported (Xie et al., 2022). The porous nature of the magnesite also influences arsenic uptake during pore filling.

In future research on calcined magnesite application to remove As from drinking water sources, the pH of water should be regulated to meet the WHO guideline for drinking water of pH 8.5 (Cotruvo, 2017). The 50 g/L and 0.5 g/L should be a maximum and minimum calcined magnesite dosage respectively and should be analyzed to investigate harmful metal contents. The enhanced mechanism for As removal on calcined magnesite should also be checked by two dimensional infrared correlation spectroscopy (2D-COS) (Li et al., 2021).

5. Conclusion

In the present study, it was observed that As removal increases with increasing calcined magnesite dosage, pH and contact time. The calcined magnesite dosage of 0.05 g/L applied to water removed 5.3 mg As/L revealing a Mg^{2+}:As ratio of 10:1. The removal process of As on calcined magnesite obeys pseudo-second-order with R^2 of 1 on 5 g/L and R^2 decreased with the decrease of calcined magnesite dosage from 5 g/L to 0.5 g/L. The removal process fitted strongly in Freundlich isotherm model. The D-R isotherm model can indicate that chemical reaction controls As removal. The calcined magnesite favored the removal of both As(V) and As(III) species present in natural drinking water from Tanzania. At high pH of 10, magnesium and calcium were not significantly released in water signifying safety of calcined magnesite at higher pH.

Declaration of competing interest

The authors declare that there is no known conflict of interests regarding the work reported in this paper.

Data availability

Data will be made available on request.

Acknowledgements

The authors would like to thank Sida-UDSM bilateral program under DAFWAT project number 2235 for funding this study. Extended thanks are due to Mr. Kentaro, Zoltan and Kjell of Stockholm University for XRD, BET and SEM-EDS analysis, respectively. ALS Scandinavia is appreciated for As speciation using HPLC-ICP-MS. Sincere thanks to Agniezska of SEED laboratory KTH for permission to use SEED laboratory facilities and ICP-OES. Special thanks to Jon-Petter of SLU for help on water sample analysis using ICP-OES at SEED Lab. My acknowledgement to Joydeep and Salam of FNM lab KTH for ICP-OES training and valuable discussions during visiting. Special thanks to the Department of Water Resources Engineering at UDSM-Tanzania for the assistance during field work for water sampling and magnesite collection.

Appendix A. Supplementary data

Supplementary data to this article can be found online at https://doi.org/10.1016/j.apgeochem.2023.105705.

References

Ahmad, A., Richards, L.A., Bhattacharya, P., 2017. Arsenic remediation of drinking water: an overview. In: Best Practice Guide on the Control of Arsenic in Drinking Water. Metals and Related Substances in Drinking Water Series. IWA publishing, pp. 79–98. https://doi.org/10.2166/9781780404929_079.

Ahmad, A., Cornelissen, E., van de Wetering, S., van Dijk, T., van Genuchten, C., Bundschuh, J., van der Wal, A., Bhattacharya, P., 2018. Arsenite removal in groundwater treatment plants by sequential Permanganate–Ferric treatment. J. Water Process Eng. 26, 221–229. https://doi.org/10.1016/j.jwpe.2018.10.014.

Ahoulé, D.G., Lalanne, F., Mendret, J., Brosillon, S., Maïga, A.H., 2015. Arsenic in african waters: a review. Water Air Soil Pollut. 226 https://doi.org/10.1007/s11270-015-2558-4.

Almås, Å.R., Manoko, M.L.K., 2012. Trace element concentrations in soil, sediments, and waters in the vicinity of Geita gold mines and north Mara gold mines in northwest Tanzania. Soil Sediment Contam. 21, 135–159. https://doi.org/10.1080/15320383.2012.649372.

Aredes, S., Klein, B., Pawlik, M., 2013. The removal of arsenic from water using natural iron oxide minerals. J. Clean. Prod. 60, 71–76. https://doi.org/10.1016/j.jclepro.2012.10.035.

Ayoob, S., Gupta, A.K., Bhakat, P.B., 2007. Performance evaluation of modified calcined bauxite in the sorptive removal of arsenic(III) from aqueous environment. Colloids Surfaces A Physicochem. Eng. Asp. 293, 247–254. https://doi.org/10.1016/j.colsurfa.2006.07.039.

Bakatula, E.N., Molaudzi, R., Nekhunguni, P., Tutu, H., 2017. The removal of arsenic and uranium from aqueous solutions by sorption onto iron oxide-coated zeolite (IOCZ). Water. Air. Soil Pollut. 228 https://doi.org/10.1007/s11270-016-3190-.

Bhakat, P.B., Gupta, A.K., Ayoob, S., Kundu, S., 2006. Investigations on arsenic(V) removal by modified calcined bauxite. Colloids Surfaces A Physicochem. Eng. Asp. 281, 237–245. https://doi.org/10.1016/j.colsurfa.2006.02.045.

Bhattacharya, P., Chatterjee, D., Jacks, G., 1997. Occurrence of arsenic-contaminated groundwater in alluvial aquifers from delta plains, eastern India: options for safe drinking water supply. Int. J. Water Resour. Dev. 13, 79–92. https://doi.org/10.1080/07900629749944.

Bhattacharya, P., Jacks, G., Ahmed, K.M., Routh, J., Khan, A.A., 2002. Arsenic in groundwater of the bengal delta plain aquifers in Bangladesh. Bull. Environ. Contam. Toxicol. 69, 538–545. https://doi.org/10.1007/s00128-002-0095-5.

Bhattacharya, P., Welch, A.H., Ahmed, K.M., Jacks, G., Naidu, R., 2004. Arsenic in groundwater of sedimentary aquifers. Appl. Geochem. 19, 163–167. https://doi.org/10.1016/j.apgeochem.2003.09.004.

Bhattacharya, P., Welch, A.H., Stollenwerk, K.G., McLaughlin, M.J., Bundschuh, J., Panaullah, G., 2007. Arsenic in the environment: biology and chemistry. Sci. Total Environ. 379, 109–120. https://doi.org/10.1016/j.scitotenv.2007.02.037.

Bulut, Y., Tez, Z., 2007. Adsorption studies on ground shells of hazelnut and almond. J. Hazard Mater. 149, 35–41. https://doi.org/10.1016/j.jhazmat.2007.03.044.

Chakraborty, S., Dasgupta, J., Farooq, U., Sikder, J., Drioli, E., Curcio, S., 2014. Experimental analysis, modeling and optimization of chromium (VI) removal from

aqueous solutions by polymer-enhanced ultrafiltration. J. Membr. Sci. 456, 139–154. https://doi.org/10.1016/j.memsci.2014.01.016.
Chiban, M., Soudani, A., Sinan, F., Persin, M., 2011. Single, binary and multi-component adsorption of some anions and heavy metals on environmentally friendly Carpobrotus edulis plant. Colloids Surf. B Biointerfaces 82, 267–276. https://doi.org/10.1016/j.colsurfb.2010.09.013.
Cotruvo, J.A., 2017. WHO guidelines for drinking water quality: first addendum to the fourth edition. J. Am. Water Works Assoc. 109, 44–51. https://doi.org/10.5942/jawwa.2017.109.0087.
Duker, A.A., Carranza, E.J.M., Hale, M., 2005. Arsenic geochemistry and health. Environ. Int. 31, 631–641. https://doi.org/10.1016/j.envint.2004.10.020.
Finkelman, R.B., 2004. Potential health impacts of burning coal beds and waste banks. Int. J. Coal Geol. 59, 19–24. https://doi.org/10.1016/j.coal.2003.11.002.
Flanagan, S.V., Johnston, R.B., Zheng, Y., 2012. Arsenic in tube well water in Bangladesh: health and economic impacts and implications for arsenic mitigation. Bull. World Health Organ. 90, 839–846. https://doi.org/10.2471/BLT.11.101253.
Gbaruko, B.C., Ana, G.R.E.E., Nwachukwu, J.K., 2008. Ecotoxicology of arsenic in the hydrosphere: implications for public health. Afr. J. Biotechnol. 7, 4737–4742. https://doi.org/10.5897/AJB08.033.
Guo, H., Stüben, D., Berner, Z., 2007. Removal of arsenic from aqueous solution by natural siderite and hematite. Appl. Geochem. 22, 1039–1051. https://doi.org/10.1016/j.apgeochem.2007.01.004.
Gupta, S.K., Chen, K.Y., 1978. Arsenic removal by adsorption. J. Water Pollut. Control Fed. 50, 493–506.
Gustafsson, J.P., Bhattacharya, P., 2007. Geochemical Modelling of Arsenic Adsorption to Oxide Surfaces, vol. 9, pp. 159–206. https://doi.org/10.1016/S0927-5215(06)09006-0.
Irunde, R., Ijumulana, J., Ligate, F., Maity, J.P., Ahmad, A., Mtamba, J., Mtalo, F., Bhattacharya, P., 2022. Arsenic in Africa: potential sources, spatial variability, and the state of the art for arsenic removal using locally available materials. Groundw. Sustain. Dev. 18, 100746 https://doi.org/10.1016/j.gsd.2022.100746.
Islam, A.B.M.R., Maity, J.P., Bundschuh, J., Chen, C.Y., Bhowmik, B.K., Tazaki, K., 2013. Arsenic mineral dissolution and possible mobilization in mineral-microbe-groundwater environment. J. Hazard Mater. 262, 989–996. https://doi.org/10.1016/j.jhazmat.2012.07.022.
Jain, C.K., Ali, I., 2000. Arsenic: occurrence, toxicity, and speciation techniques. Water Res. 34, 4304–4312. https://doi.org/10.1016/S0043-1354(00)00182-2.
Kassenga, G., Mato, R., 2008. Arsenic contamination levels in drinking water sources in mining areas in Lake Victoria Basin, Tanzania, and its removal using stabilized ferralsols. Int. J. Biol. Chem. Sci. 2, 389–400. https://doi.org/10.4314/ijbcs.v2i4.39771.
Kıpçak, İ., Isıyel, T.G., 2015. Magnesite tailing as low-cost adsorbent for the removal of copper (II) ions from aqueous solution. Kor. J. Chem. Eng. 32, 1634–1641. https://doi.org/10.1007/s11814-014-0377-8.
Ladeira, A.C.Q., Ciminelli, V.S.T., 2004. Adsorption and desorption of arsenic on an oxisol and its constituents. Water Res. 38, 2087–2094. https://doi.org/10.1016/j.watres.2004.02.002.
Li, X., Yan, L., Zhong, W., Kersten, M., Jing, C., 2021. Competitive arsenate and phosphate adsorption on α-FeOOH, LaOOH, and nano-TiO2: two-dimensional correlation spectroscopy study. J. Hazard Mater. 414, 125512 https://doi.org/10.1016/j.jhazmat.2021.125512.
Liang, H., Guo, P., Yang, Y., Wang, W., Sun, Z., 2022. Environmental application of engineering magnesite slag for phosphate adsorption from wastewater. Environ. Sci. Pollut. Res. 29, 59502–59512. https://doi.org/10.1007/s11356-022-20029-z.
Ligate, F., Lucca, E., Ijumulana, J., Irunde, R., Kimambo, V., Mtamba, J., Ahmad, A., Hamisi, R., Prakash, J., Mtalo, F., 2022. Geogenic contaminants and groundwater quality around Lake Victoria goldfields in northwestern Tanzania. Chemosphere 307, 135732. https://doi.org/10.1016/j.chemosphere.2022.135732.
Litter, M.I., Ingallinella, A.M., Olmos, V., Savio, M., Difeo, G., Botto, L., Torres, E.M.F., Taylor, S., Frangie, S., Herkovits, J., Schalamuk, I., González, M.J., Berardozzi, E., García Einschlag, F.S., Bhattacharya, P., Ahmad, A., 2019. Arsenic in Argentina: technologies for arsenic removal from groundwater sources, investment costs and waste management practices. Sci. Total Environ. 690, 778–789. https://doi.org/10.1016/j.scitotenv.2019.06.358.
Liu, Jing, Huang, X., Liu, Juan, Wang, W., Zhang, W., Dong, F., 2014. Adsorption of arsenic(V) on bone char: batch, column and modeling studies. Environ. Earth Sci. 72, 2081–2090. https://doi.org/10.1007/s12665-014-3116-x.
Lucca, E., 2017. Geochemical investigation of arsenic in drinking water sources in proximity of gold mining areas within the lake victoria basin, in northern Tanzania. TRITA SEED-EX 2017 25, 99. https://kth.diva-portal.org/smash/record.jsf?pid=diva2%3A1189665&dswid=-3449.
Maity, J.P., Ho, P.R., Huang, Y.H., Sun, A.C., Chen, C.C., Chen, C.Y., 2019. The removal of arsenic from arsenic-bearing groundwater in In-situ and Ex-situ environment using novel natural magnetic rock material and synthesized magnetic material as adsorbent: a comparative assessment. Environ. Pollut. 253, 768–778. https://doi.org/10.1016/j.envpol.2019.07.048.
Maity, J.P., Chen, C.Y., Bhattacharya, P., Sharma, R.K., Ahmad, A., Patnaik, S., Bundschuh, J., 2021. Advanced application of nano-technological and biological processes as well as mitigation options for arsenic removal. J. Hazard Mater. 405, 123885 https://doi.org/10.1016/j.jhazmat.2020.123885.
Maji, S.K., Pal, A., Pal, T., 2008. Arsenic removal from real-life groundwater by adsorption on laterite soil. J. Hazard Mater. 151, 811–820. https://doi.org/10.1016/j.jhazmat.2007.06.060.
Mandal, K.B., Suzuki, T.K., 2002. Arsenic round the world: a review. Talanta 58, 201–235. https://doi.org/10.1016/S0039-9140(02)00268-0.
Masindi, V., 2021. Conversion of cryptocrystalline magnesite to MgO nanosheets: insights into microstructural properties. Mater. Today: Proc. 38, 1077–1087.
Masindi, V., Gitari, W.M., 2016. Removal of arsenic from wastewaters by cryptocrystalline magnesite: complimenting experimental results with modelling. J. Clean. Prod. 113, 318–324. https://doi.org/10.1016/j.jclepro.2015.11.043.
Masindi, V., Gitari, M.W., Tutu, H., De Beer, M., 2014. Application of magnesite–bentonite clay composite as an alternative technology for removal of arsenic from industrial effluents. Toxicol. Environ. Chem. 96, 1435–1451. https://doi.org/10.1080/02772248.2014.966714.
McNeill, L.S., Edwards, M., 1997. Arsenic removal during precipitative softening. J. Environ. Eng. 123, 453–460. https://doi.org/10.1061/(asce)0733-9372(1997)123:5(453).
Mishra, S.P., Mohapatra, D., Mishra, D., Chattopadhyay, P., Roy Chaudhury, G., Das, R.P., 2014. Arsenic adsorption on natural minerals. J. Mater. Environ. Sci. 5, 350–359.
Mohan, D., Pittman, C.U., 2007. Arsenic removal from water/wastewater using adsorbents-A critical review. J. Hazard Mater. 142, 1–53. https://doi.org/10.1016/j.jhazmat.2007.01.006.
Mohapatra, D., Mishra, D., Chaudhury, G.R., Das, R.P., 2006. Effect of dissolved organic matter on the adsorption and stability of As(V) on manganese wad. Sep. Purif. Technol. 49, 223–229. https://doi.org/10.1016/j.seppur.2005.10.003.
Mohapatra, D., Mishra, D., Chaudhury, G.R., Das, R.P., 2007. An investigation into the prospects of arsenic(v) removal from contaminated groundwater using untreated bauxite ore. J. Environ. Sci. Heal. - Part A Toxic/Hazardous Subst. Environ. Eng. 42, 831–838. https://doi.org/10.1080/10934520701304948.
Mulana, F., Mustanir, Fuadi, Z., 2019. Synthesis of Kieserite fertilizer by using natural magnesite Ore as raw material. IOP Conf. Ser. Mater. Sci. Eng. 523 https://doi.org/10.1088/1757-899X/523/1/012019.
Natsi, P.D., Goudas, K.-A., Koutsoukos, P.G., 2023. Phosphorus recovery from municipal wastewater: brucite from MgO hydrothermal treatment as magnesium source. Crystals 13, 208. https://doi.org/10.3390/cryst13020208.
Nyanza, E.C., Dewey, D., Thomas, D.S.K., Davey, M., Ngallaba, S.E., 2014. Spatial distribution of mercury and arsenic levels in water, soil and cassava plants in a community with long history of gold mining in Tanzania. Bull. Environ. Contam. Toxicol. 93, 716–721. https://doi.org/10.1007/s00128-014-1315-5.
Nyanza, E.C., Bernier, F.P., Manyama, M., Hatfield, J., Martin, J.W., Dewey, D., 2019. Maternal exposure to arsenic and mercury in small-scale gold mining areas of Northern Tanzania. Environ. Res. 173, 432–442. https://doi.org/10.1016/j.envres.2019.03.0317.
Paikaray, S., Essilfie-Dughan, J., Hendry, M.J., 2018. Ionic substitution of Mg2+ for Al3+ and Fe3+ with octahedral coordination in hydroxides facilitate precipitation of layered double hydroxides. Geochem. Cosmochim. Acta 220, 217–234. https://doi.org/10.1016/j.gca.2017.10.003.
Raj, D., Maiti, S.K., 2020. Sources, bioaccumulation, health risks and remediation of potentially toxic metal(loid)s (As, Cd, Cr, Pb and Hg): an epitomised review. Environ. Monit. Assess. 192, 108. https://doi.org/10.1007/s10661-019-8060-5.
Rango, T., Vengosh, A., Dwyer, G., Bianchini, G., 2013. Mobilization of arsenic and other naturally occurring contaminants in groundwater of the main ethiopian rift aquifers. Water Res. 47, 5801–5818. https://doi.org/10.1016/j.watres.2013.07.002.
Rukh, S., Akhtar, M.S., Mehmood, A., Hassan, S., Khan, K.S., Naqvi, S.M.S., Imran, M., 2017. Arsenate and arsenite adsorption in relation with chemical properties of alluvial and loess soils. J. Serb. Chem. Soc. 82, 943–954. https://doi.org/10.2298/JSC170209042R.
Sadik, C., Moudden, O., El Bouari, A., El Amrani, I.E., 2016. Review on the elaboration and characterization of ceramics refractories based on magnesite and dolomite. J. Asian Ceram. Soc. 4, 219–233. https://doi.org/10.1016/j.jascer.2016.06.006.
Salameh, Y., Albadarin, A.B., Allen, S., Walker, G., Ahmad, M.N.M., 2015. Arsenic(III,V) adsorption onto charred dolomite: charring optimization and batch studies. Chem. Eng. J. 259, 663–671. https://doi.org/10.1016/j.cej.2014.08.038.
Sanou, Y., Pare, S., 2021. Comparative Study of Adsorption Capacity of Two Mixed Materials for Arsenic Remediation, vol. 9, pp. 559–565.
Shadrunova, I.V., Orekhova, N.N., Stefunko, M.S., 2022. Intensification of the wastewater treatment process using magnesium-containing materials. IOP Conf. Ser. Earth Environ. Sci. 1061, 0–8. https://doi.org/10.1088/1755-1315/1061/1/012029.
Simsek, E.B., Beker, U., 2014. Kinetic performance of aluminum and iron oxides in the removal of arsenate from aqueous environment. J. Clean Energy Technol. 2, 206–209. https://doi.org/10.7763/jocet.2014.v2.124.
Smith, A.H., Hopenhayn-Rich, C., Bates, M.N., Goeden, H.M., Hertz-Picciotto, I., Duggan, H.M., Wood, R., Kosnett, M.J., Smith, M.T., 1992. Cancer risks from arsenic in drinking water. Environ. Health Perspect. 97, 259–267. https://doi.org/10.1289/ehp.9297259.
Tahmasebpoor, M., Hosseini Nami, S., Khatamian, M., Sanaei, L., 2022. Arsenate removal from contaminated water using Fe2O3-clinoptilolite powder and granule. Environ. Technol. 43, 116–130. https://doi.org/10.1080/09593330.2020.1779821.
Taylor, H., Appleton, J.D., Lister, R., Smith, B., Chitamweba, D., Mkumbo, O., Machiwa, J.F., Tesha, A.L., Beinhoff, C., 2005. Environmental assessment of mercury contamination from the Rwamagasa artisanal gold mining centre, Geita District, Tanzania. Sci. Total Environ. 343, 111–133. https://doi.org/10.1016/j.scitotenv.2004.09.042.
Tong, L., Tang, M., 1999. Expansion mechanism of alkali-dolomite and alkali-magnesite reaction. Cem. Concr. Compos. 21, 361–373. https://doi.org/10.1016/S0958-9465(99)00022-0.
Violante, A., Cozzolino, V., Perelomov, L., Caporale, A.G., Pigna, M., 2010. Mobility and bioavailability of heavy metals and metalloids in soil environments. J. Soil Sci. Plant Nutr. 10, 268–292. https://doi.org/10.4067/S0718-95162010000100005.

Wang, Z., Shen, X., Jing, M., Li, C., 2018. Enhanced arsenic removal from drinking water by FeOOH/γ-Al2O3 granules. J. Alloys Compd. 735, 1620–1628. https://doi.org/10.1016/j.jallcom.2017.11.284.

Wei, J., Ge, J., Rouff, A.A., Wen, X., Meng, X., Song, Y., 2019. Phosphorus recovery from wastewater using light calcined magnesite, effects of alkalinity and organic acids. J. Environ. Chem. Eng. 7, 103334 https://doi.org/10.1016/j.jece.2019.103334.

Wu, C., Liu, W., Zhang, J., Chu, S., Shi, Z., Dang, Z., Lin, Z., 2017. Mechanisms of synergistic removal of low concentration As(V) by nZVI@Mg(OH)2 nanocomposite. J. Phys. Chem. C 121, 21411–21419. https://doi.org/10.1021/acs.jpcc.7b06356.

Xie, X., Lu, C., Xu, R., Yang, X., Yan, L., Su, C., 2022. Arsenic removal by manganese-doped mesoporous iron oxides from groundwater: performance and mechanism. Sci. Total Environ. 806, 150615 https://doi.org/10.1016/j.scitotenv.2021.150615.

Xu, Y., Dai, Y., Zhou, J., Xu, Z.P., Qian, G., Lu, G.Q.M., 2010. Removal efficiency of arsenate and phosphate from aqueous solution using layered double hydroxide materials: intercalation vs. precipitation. J. Mater. Chem. 20, 4684–4691. https://doi.org/10.1039/b926239c.

Zhang, W., Singh, P., Paling, E., Delides, S., 2004. Arsenic removal from contaminated water by natural iron ores. Miner. Eng. 17, 517–524. https://doi.org/10.1016/j.mineng.2003.11.020.

Zhang, T., Zhao, Y., Kang, S., Bai, H., Song, G., Zhang, Q., 2021. Enhanced Arsenic Removal from Water by Mechanochemical Synthesis of Ca–Al–Fe Ternary Co.

Zhao, K., Guo, H., Zhou, X., 2014. Adsorption and heterogeneous oxidation of arsenite on modified granular natural siderite: characterization and behaviors. Appl. Geochem. 48, 184–192. https://doi.org/10.1016/j.apgeochem.2014.07.016.

Appendix A. Supplementary Data

The natural magnesite efficacy on arsenic extraction from water and alkaline influence on metal release in water

Regina Irunde[1,2,3*], Fanuel J. Ligate[1,2,5], Julian Ijumulana[1,2,4], Arslan Ahmad[1,7], Jyoti Prakash Maity[6], Rajabu Hamis[1], Joseph Y.N. Philip[3], Kessy Fidel Kilulya[3], Erik Karltun[8], Joseph Mtamba[2], Prosun Bhattacharya[1], Felix Mtalo[2]

[1]*KTH-International Groundwater Arsenic Research Group, Department of Sustainable Development, Environmental Science and Engineering, KTH Royal Institute of Technology, Teknikringen 10B, SE-100 44 Stockholm, Sweden*

[2]*Department of Water Resources Engineering, College of Engineering and Technology, University of Dar es Salaam, Dar es Salaam, Tanzania*

[3]*Department of Chemistry, College of Natural and Applied Sciences, University of Dar es Salaam, Tanzania*

[4]*Department of Transportation and Geotechnical Engineering, College of Engineering and Technology, University of Dar es Salaam, Tanzania*

[5]*Department of Chemistry, Mkwawa College of Education, University of Dar es Salaam, Tanzania.*

[6]*Department of Chemistry, School of Applied Sciences, KIIT Deemed to be University, Bhubaneswar, Odisha 751024, India.*

[7]*SIBELCO Ankerpoort NV, Op de Bos 300, 6223 EP Maastricht, The Netherlands.*

[8]*Department of Soil and Environment, Swedish University of Agricultural Sciences, SLU, P.O. Box 7014, SE-750 07 Uppsala, Sweden.*

S1. XRD

Table S1a. Calcined magnesite powder, some peak pattern selected from Xpert HigScore plus version 3.05 ICDD PDF-4+ 2022. MgO and Fe_2O_3 were included under restriction set

Visible	Ref. Code	Score	Compound Name	Displacement [°2Th.]	Scale Factor	Chemical Formula
*	04-023-8811	83	Magnesium Iron Carbonate	0.147	0.990	$Mg_{0.99}Fe_{0.01}(CO_3)$
*	00-002-0871	43	Magnesium Carbonate	0.114	0.771	$MgCO_3$
*	04-022-6948	54	Iron Carbonate	0.120	1.003	$Fe(CO_3)$
*	01-077-8621	13	Silicon Oxide	-0.026	0.061	SiO_2
*	00-019-0771	0	Magnesium Oxide	0.125	0.183	MgO_2
*	01-080-4190	1	Magnesium Oxide	-0.049	3.353	MgO
*	01-088-3891	12	Iron Oxide	-0.157	0.538	Fe_2O_3

Table S1b. Calcined magnesite powder, Peak list selected phases from the database. MgO and Fe_2O_3 under restriction is included

Pos. [°2Th.]	Height [cts]	FWHM Left [°2Th.]	d-spacing [Å]	Rel. Int. [%]	Tip Width	Matched by
21.0598	14.55	0.3744	4.21508	2.00	0.4493	01-077-8621; 01-080-4190
26.7393	56.67	0.1248	3.33128	7.77	0.1498	01-077-8621
32.8073	729.12	0.2184	2.72767	100.00	0.2621	04-023-8811; 00-002-0871; 04-022-6948; 01-088-3891
35.9410	110.75	0.2184	2.49670	15.19	0.2621	04-023-8811; 00-002-0871; 04-022-6948; 01-088-3891
38.9780	45.67	0.2496	2.30887	6.26	0.2995	04-023-8811; 04-022-6948
43.0967	534.06	0.1872	2.09727	73.25	0.2246	04-023-8811; 00-002-0871; 04-022-6948; 01-080-4190
46.9191	126.69	0.2496	1.93493	17.38	0.2995	04-023-8811; 04-022-6948
51.7425	48.67	0.2184	1.76532	6.68	0.2621	04-023-8811; 00-002-0871; 04-022-6948
54.0256	413.15	0.2184	1.69599	56.66	0.2621	04-023-8811; 00-002-0871; 04-022-6948; 00-019-0771
60.1148	25.04	0.1872	1.53793	3.43	0.2246	01-077-8621
61.4971	72.26	0.2184	1.50663	9.91	0.2621	04-023-8811; 00-002-0871; 04-022-6948; 01-080-4190
62.5363	118.59	0.1872	1.48407	16.27	0.2246	04-023-8811; 00-002-0871; 04-022-6948; 01-080-4190
66.5119	81.95	0.1872	1.40468	11.24	0.2246	04-023-8811; 04-022-6948; 01-088-3891
68.4829	37.24	0.1872	1.36898	5.11	0.2246	04-023-8811; 00-002-0871; 04-022-6948; 01-077-8621
69.4456	113.04	0.1872	1.35234	15.50	0.2246	04-023-8811; 04-022-6948
70.4579	164.15	0.2184	1.33536	22.51	0.2621	04-023-8811; 00-002-0871; 04-022-6948; 01-088-3891
76.0816	54.62	0.1872	1.25003	7.49	0.2246	04-023-8811; 00-002-0871; 01-077-8621
77.0246	36.69	0.1872	1.23707	5.03	0.2246	04-023-8811; 00-002-0871; 04-022-6948

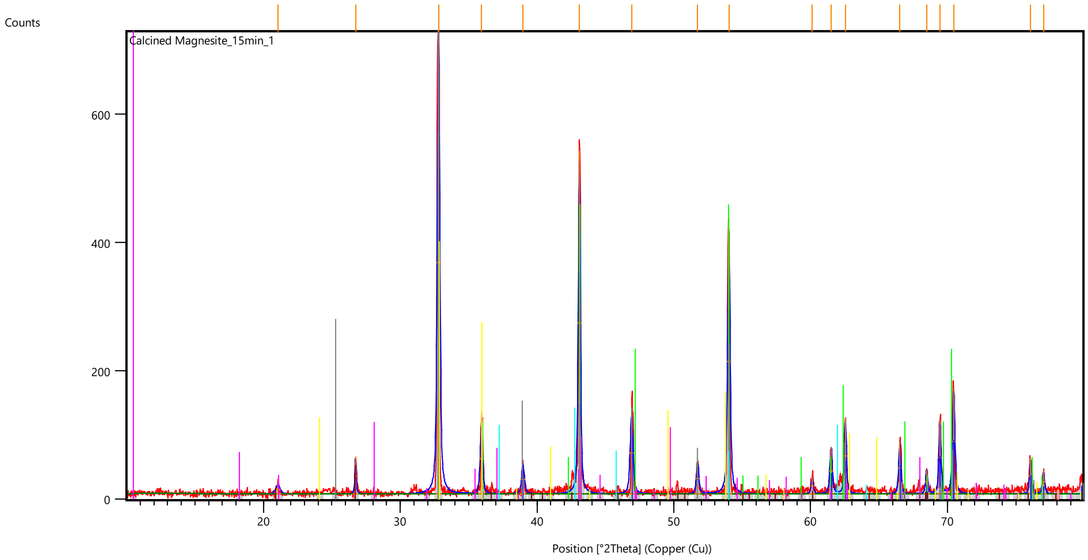

Figure S1a. Calcined magnesite at 500°C

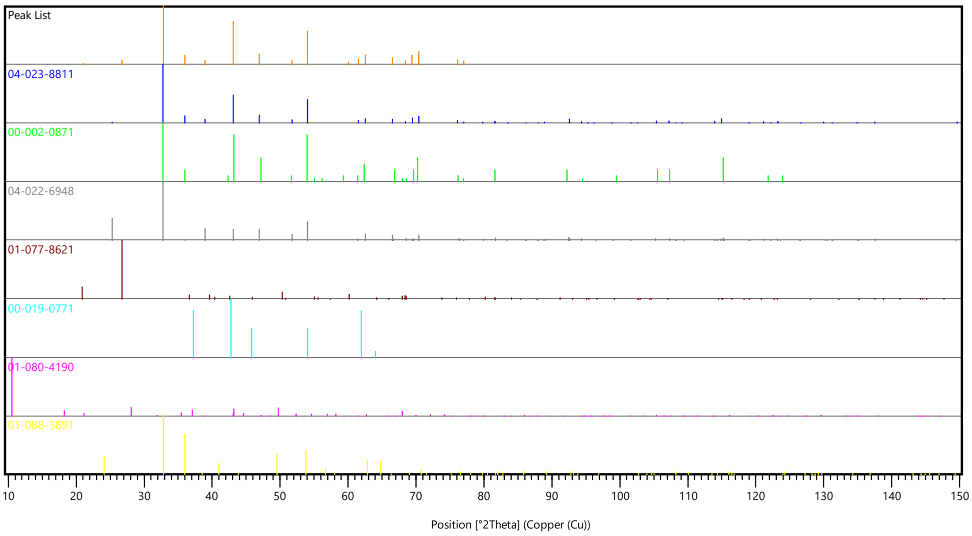

Figure S1b. XRD showing selected phase list for Table S1 and figure S1a

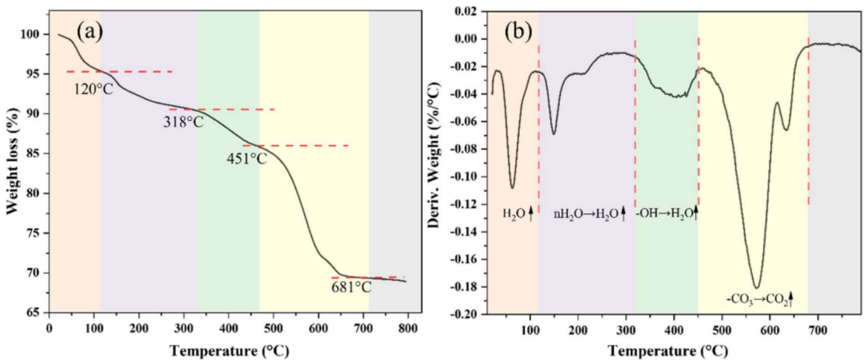

Figure S2. TG curves for phosphate adsorption on magnesite (Liang et al., 2022) TGA reported to decrease in mass as temperature increases due to loss of water.

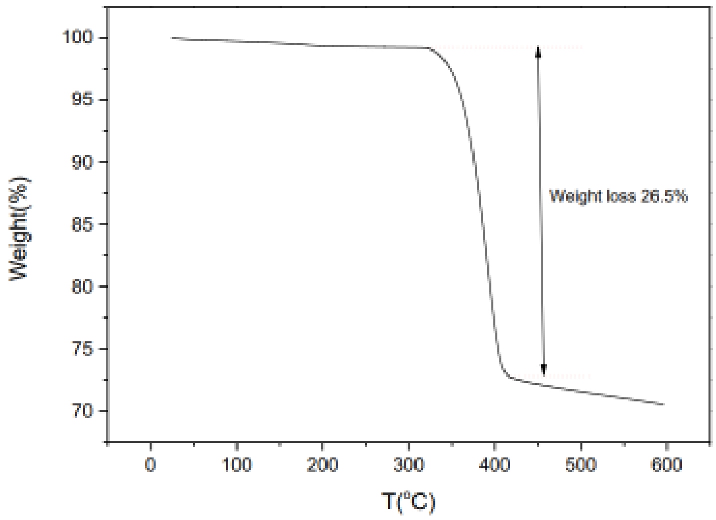

Figure S3. MgO pure powder rises pH to 13-14 (Natsi et al., 2023)

S.2 Effect of pH on arsenic removal

Preliminary pH investigation using distilled water of pH 5.71, regulated by 10 drops 0.1M HCL to pH 1.51. The 200 g/L added in this pH 1.51, shaked for 5 minutes resulted pH of 10.62

Table S2. Effect of magnesite dosage on pH raise

Time (min)	pH with magnesite dosage				Time (min)	pH with magnesite dosage
	0.002 g/L	0.0055 g/L	0.0155 g/L	0.05 g/L		100 g/L
0	6.8	6.8	6.8	6.8	0	1.47
5	7.25	7.43	7.77	9.82	20	10.22
15	7.25	7.36	8.22	9.72	40	10.51
30	7.34	7.24	8.47	10.19	60	10.48
60	7.4	7.37	8.76	10.31	80	10.29
120	7.42	7.42	8.33	10.09	120	10.18
180	7.26	7.42	8.72	10.32	160	9.96
					180	10.31
					240	10.18

S3. Visual MINTEQ version 3.1

Table S3. Removal efficiency from natural water simulated in Visual MINTEQ

	% sorbed at different levels of calcined magnesite dosage (g/L)									
Species	**0.001**	**0.005**	**0.008**	**0.01**	**0.03**	**0.09**	**5.0**	**10.0**	**20.0**	**30.0**
AsO_4^{3-}	3.302	17.939	30.653	40.092	99.97	99.998	100	100	100	100
Ca^{2+}	0.003	0.016	0.025	0.031	0.018	0.056	19.484	39.992	67.289	80.264
Cd^{2+}	0.438	2.243	3.648	4.609	12.376	31.459	98.806	99.432	99.734	99.824
Cl^{-}	0	0	0	0	0.001	0.008	0.329	0.666	1.405	2.243
Co^{2+}	0.37	1.901	3.102	3.928	10.458	27.316	98.615	99.401	99.752	99.849
CO_3^{2-}	0.001	0.006	0.01	0.014	0.996	7.037	85.332	92.466	96.422	97.756
Cu^{2+}	0.978	4.513	6.939	8.475	17.983	32.005	80.932	88.059	92.841	94.702
Fe^{2+}	0.38	1.957	3.199	4.057	12.192	32.774	98.621	99.411	99.772	99.874
H^{+}	1.595	6.142	8.405	9.607	22.864	50.701	104.831	102.034	101.03	100.765
H_3AsO_3	0.753	4.124	7.164	9.555	90.156	98.61	99.981	99.991	99.996	99.997
$HSeO_3^{-}$	0.009	0.052	0.1	0.145	57.222	94.453	99.904	99.956	99.981	99.989
Li^{+}	0	0.001	0.002	0.002	0	0	0	0	0	0
Mg^{2+}	0.012	0.063	0.102	0.129	0.305	0.969	53.427	70.934	83.981	89.069
Mn^{2+}	0.134	0.699	1.152	1.467	4.137	12.673	98.803	99.577	99.871	99.938
Ni^{2+}	1.16	5.779	9.203	11.462	27.173	54.764	99.736	99.895	99.959	99.976
NO_3^{-}	0	0	0	0	0.001	0.008	0.329	0.666	1.405	2.243
Pb^{2+}	25.286	63.462	73.843	78.098	91.682	97.262	99.989	99.995	99.998	99.998
PO_4^{3-}	5.62	27.739	43.849	54.291	99.979	99.999	100	100	100	100
SO_4^{2-}	0	0	0	0	0.033	0.396	19.33	35.171	57.93	71.547
Sr^{2+}	0.003	0.015	0.023	0.028	0.005	0.015	17.899	38.832	67.385	80.723

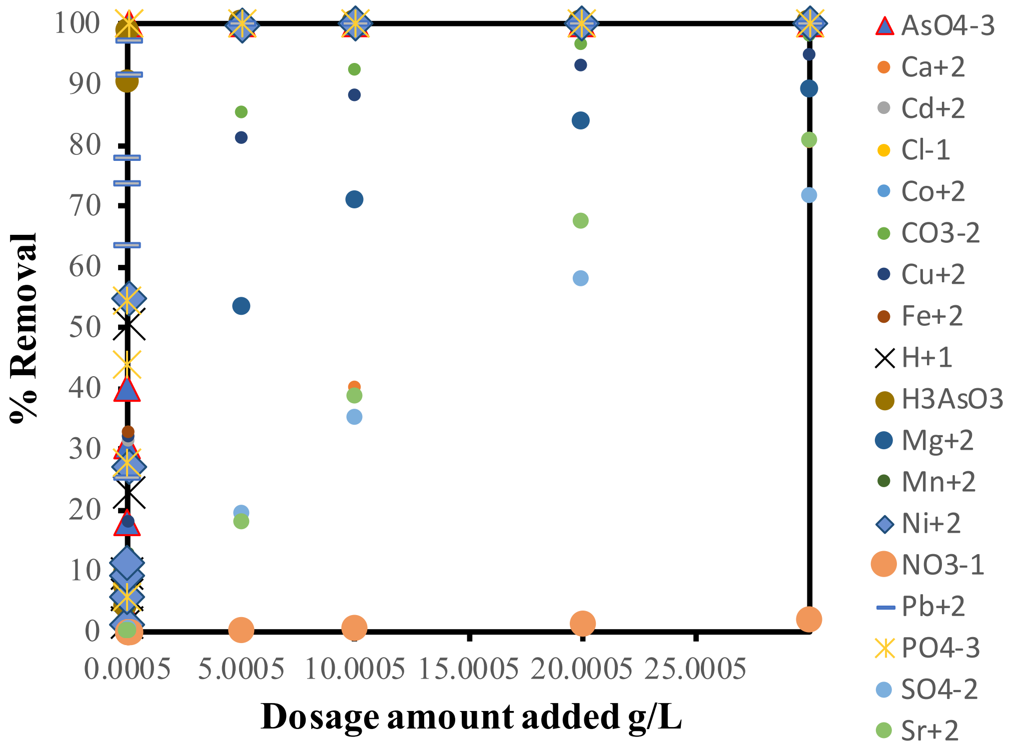

Figure S4. Arsenic trend removal from natural water simulated by Visual minteq

S4. Saturation indices

Table S4. Saturation indices in natural water when 5g/L $MgCO_3$ involved

5g/L MgCO3	pH4	pH6.8	pH 10	pH 12	pH 13
Mineral pH 6.8	Sat. index	Sat. index	Sat. index	Sat. index	Sat. index
Anglesite	-4.47	-8.782	-10.211	-10.927	-13.56
Anhydrite	-2.6	-2.607	-2.649	-2.705	-2.944
Antlerite	-18.249	-17.508	-11.758	-13.179	-18.73
Aragonite	-4.934	-0.298	1.855	2.016	2.079
Arsenolite	-14.175	-16.038	-21.477	-21.704	-22.042
Artinite	-13.878	-3.668	4.614	8.372	9.467
$As_2O_5(s)$	-29.829	-36.333	-58.006	-65.781	-68.595
Atacamite	-13.58	-12.192	-7.355	-7.721	-11.184
Azurite	-16.124	-11.624	-7.74	-12.553	-19.336
Brochantite	-24.023	-21.192	-11.441	-12.059	-18.848
Brucite	-10.354	-4.807	1.362	5.044	6.361
$Ca_3(AsO_4)_2$:$4H_2O(s)$	-32.179	-22.12	-25.152	-21.614	-19.634
$Ca_3(PO_4)_2$ (am1)	-25.62	-15.502	-12.42	-5.138	-2.83
$Ca_3(PO_4)_2$ (am2)	-22.87	-12.752	-9.67	-2.388	-0.08
$Ca_3(PO_4)_2$ (beta)	-22.2	-12.082	-9	-1.718	0.59
$Ca_4H(PO_4)_3$:$3H_2O(s)$	-30.996	-18.578	-17.054	-8.011	-5.353
$CaCO_3xH_2O(s)$	-6.132	-1.495	0.659	0.821	0.883
$CaHPO_4(s)$	-8.532	-6.233	-7.797	-6.04	-5.686
$CaHPO_4$:$2H_2O(s)$	-8.824	-6.525	-8.085	-6.326	-5.975
Calcite	-4.79	-0.154	1.999	2.16	2.223
$CaMoO_4(s)$	-7.315	-3.931	-3.969	-3.847	-3.802
$CaSeO_4$:$2H_2O(s)$	-7.824	-7.796	-7.973	-8.171	-8.599
$Cd(OH)_2(s)$	-14.124	-9.62	-4.806	-1.599	-1.686
$Cd_3(OH)_4SO_4(s)$	-35.442	-27.458	-19.271	-13.475	-15.575
$Cd_3(PO_4)_2(s)$	-33.406	-26.339	-27.454	-21.862	-24.611
$Cd_3OH_2(SO_4)_2(s)$	-31.034	-28.578	-26.646	-24.677	-28.614
Cd_4(OH)6SO4(s)	-41.762	-29.275	-16.273	-7.27	-9.457
$CdCl_2(s)$	-14.841	-15.918	-17.438	-18.17	-20.232
$CdCl_2$:$1H_2O(s)$	-13.812	-14.89	-16.407	-17.139	-19.201
$CdCl_2$:$2.5H_2O(s)$	-13.602	-14.679	-16.194	-16.923	-18.988
$CdF_2(s)$	-16.869	-17.862	-19.091	-19.478	-21.105
$CdMoO_4(s)$	-6.078	-3.71	-5.147	-5.588	-7.23
CdOHCl(s)	-11.527	-9.814	-8.167	-6.929	-8.004
$CdSeO_4$:$2H_2O(s)$	-13.956	-14.946	-16.521	-17.282	-19.396
$CdSO_4(s)$	-11.75	-12.774	-14.215	-14.834	-16.759
$CdSO_4$:$1H_2O(s)$	-10.202	-11.226	-12.665	-13.283	-15.209
$CdSO_4$:$2.67H_2O(s)$	-10.065	-11.089	-12.525	-13.141	-15.069
Celestite	-2.419	-2.44	-2.325	-2.278	-2.425
Cerrusite	-5.37	-5.039	-4.274	-4.773	-7.103
Chalcanthite	-8.172	-11.609	-13.853	-16.873	-19.953
Chloropyromorphite (c)	-24.018	-30.397	-32.771	-25.232	-33.928
Chloropyromorphite(soil)	-28.048	-34.427	-36.801	-29.262	-37.958
Claudetite	-14.215	-16.078	-21.517	-21.744	-22.082

$Co(OH)_2$ (am)	-12.319	-7.254	-2.138	-1.044	-1.52
$Co(OH)_2$ (c)	-11.515	-6.45	-1.334	-0.24	-0.716
$Co_3(AsO_4)_2(s)$	-33.974	-25.285	-31.617	-36.113	-40.351
$Co_3(PO_4)_2(s)$	-27.552	-18.802	-19.014	-19.76	-23.675
$CoCl_2(s)$	-22.511	-23.028	-24.246	-27.092	-29.542
$CoCl_2:6H_2O(s)$	-16.817	-17.332	-18.54	-21.378	-23.835
$CoCO_3(s)$	-5.777	-1.597	-0.542	-3.057	-5.068
$CoF_2(s)$	-15.229	-15.661	-16.589	-19.089	-21.105
$CoHPO_4(s)$	-12.453	-10.61	-13.272	-14.191	-15.912
$CoMoO_4(s)$	-11.211	-8.283	-9.418	-11.973	-14.003
$CoO(s)$	-12.805	-7.74	-2.627	-1.533	-2.008
$Cu(OH)_2(s)$	-8.63	-6.54	-2.538	-1.736	-2.974
$CuCO_3(s)$	-5.592	-4.387	-4.446	-7.253	-10.026
Dolomite (disordered)	-7.736	1.562	5.823	6.057	5.902
Dolomite (ordered)	-7.186	2.112	6.373	6.607	6.452
Epsomite	-2.612	-2.591	-2.665	-2.801	-3.33
$Fe(OH)_2$ (am)	-14.329	-8.988	-5.455	-3.712	-3.955
$Fe(OH)_2$ (c)	-13.729	-8.388	-4.855	-3.112	-3.355
$FeMoO_4(s)$	-10.495	-7.29	-10.008	-11.915	-13.711
Fluorite	-2.619	-2.596	-2.426	-2.249	-2.191
Gypsum	-2.362	-2.368	-2.407	-2.461	-2.702
$H_2MoO_4(s)$	-6.883	-9.019	-15.266	-18.913	-20.469
Huntite	-16.32	2.303	10.781	11.159	10.567
Hydrocerrusite	-19.198	-17.32	-10.963	-8.851	-14.308
Hydromagnesite	-28.535	-4.339	10.27	14.247	14.685
Hydroxyapatite	-30.107	-12.169	-4.439	8.37	12.631
Hydroxylpyromorphite	-38.148	-41.736	-40.944	-31.435	-39.144
Langite	-26.296	-23.465	-13.711	-14.329	-21.118
Larnakite	-12.637	-15.734	-12.339	-9.946	-13.373
Laurionite	-8.95	-10.525	-8.867	-7.726	-9.509
$Li_2MoO_4(s)$	-26.374	-22.91	-22.752	-22.4	-22.085
$LiF(s)$	-8.123	-8.072	-7.889	-7.685	-7.521
Lime	-28.211	-22.691	-16.479	-12.71	-11.11
Litharge	-13.502	-12.286	-7.462	-4.353	-5.147
Magnesite	-3.546	1.116	3.225	3.297	3.079
Malachite	-10.963	-7.668	-3.725	-5.731	-9.741
Massicot	-13.702	-12.486	-7.662	-4.553	-5.347
Matlockite	-8.155	-12.478	-13.841	-14.497	-17.05
Melanothallite	-20.616	-24.108	-26.44	-29.578	-32.79
Melanterite	-10.114	-10.299	-13.009	-15.085	-17.173
$Mg(OH)_2$ (active)	-12.048	-6.501	-0.332	3.35	4.667
$Mg_2(OH)_3Cl:4H_2O(s)$	-20.041	-11.738	-2.56	2.839	4.481
$Mg_3(PO_4)_2(s)$	-21.047	-10.851	-7.903	-0.886	0.577
$MgCO_3:5H_2O(s)$	-6.496	-1.833	0.285	0.363	0.138
$MgF_2(s)$	-2.745	-2.695	-2.57	-2.482	-2.705
$MgHPO_4:3H_2O(s)$	-7.386	-5.061	-6.663	-4.991	-4.923
$MgMoO_4(s)$	-11.151	-7.741	-7.823	-7.79	-8.027

$MgSeO_4:6H_2O(s)$	-7.404	-7.35	-7.563	-7.845	-8.56
$Mn_3(AsO_4)2:8H_2O(s)$	-37.235	-28.325	-35.158	-32.309	-33.374
$Mn_3(PO_4)_2(s)$	-42.125	-33.156	-33.883	-27.294	-28.026
$MnCl_2:4H_2O(s)$	-18.221	-18.663	-20.047	-20.442	-21.836
$MnCO_3$ (am)	-7.714	-3.461	-2.578	-2.648	-3.598
$MnHPO_4(s)$	-7.351	-5.435	-8.269	-6.743	-7.403
$MnSeO_4:5H_2O(s)$	-13.756	-14.111	-15.552	-15.978	-17.423
$MnSO_4(s)$	-14.487	-14.877	-16.189	-16.476	-17.728
$MoO_3(s)$	-11.753	-13.89	-20.139	-23.786	-25.342
Morenosite	-5.899	-6.895	-8.214	-11.077	-13.904
Nesquehonite	-6.354	-1.691	0.423	0.498	0.276
$Ni(OH)_2$ (am)	-9.449	-4.92	0.004	0.96	-0.021
$Ni(OH)_2$ (c)	-7.349	-2.82	2.104	3.06	2.079
$NiCO_3(s)$	-3.111	0.534	1.397	-1.257	-3.773
$NiMoO_4(s)$	-5.164	-2.771	-4.098	-6.792	-9.327
$NiSeO_4:6H_2O(s)$	-10.389	-11.352	-12.811	-15.819	-18.832
Otavite	-6.222	-2.603	-1.849	-2.252	-3.874
$Pb(OH)_2(s)$	-8.968	-7.752	-2.926	0.184	-0.611
Periclase	-14.832	-9.285	-3.118	0.563	1.881
Phosgenite	-14.597	-18.632	-19.375	-20.703	-25.803
Portlandite	-18.222	-12.701	-6.488	-2.717	-1.119
Powellite	-7.345	-3.961	-3.999	-3.877	-3.832
Pyrochroite	-15.656	-10.518	-5.575	-2.035	-1.45
Retgersite	-5.998	-6.994	-8.315	-11.179	-14.004
Rhodochrosite	-7.214	-2.961	-2.078	-2.148	-3.098
Rutile	-0.395	-0.393	-0.415	-0.808	-1.612
Senarmontite	-2.692	-2.688	-2.737	-3.722	-5.434
$SeO_3(s)$	-36.364	-41.858	-48.249	-52.219	-54.244
Siderite	-8.001	-3.544	-4.072	-5.939	-7.716
$SrF_2(s)$	-6.618	-6.609	-6.282	-6.002	-5.852
$SrHPO_4(s)$	-10.591	-8.307	-9.713	-7.853	-7.407
$SrSeO_4(s)$	-8.511	-8.498	-8.521	-8.619	-8.952
Strontianite	-6.079	-1.458	0.853	1.116	1.272
Tenorite(am)	-7.824	-5.734	-1.734	-0.933	-2.17
Tenorite(c)	-6.974	-4.884	-0.884	-0.083	-1.32
$TlCl(s)$	-6.257	-6.249	-6.682	-6.895	-7.168
$TlNO_3(s)$	-8.023	-8.025	-8.489	-8.727	-9.019
$TlOH(s)$	-15.406	-12.608	-9.873	-8.117	-7.402
$V_2O_4(s)$	-3.203	-0.436	0.448	2.063	2.592
Valentinite	-4.132	-4.128	-4.177	-5.162	-6.874
Vaterite	-5.357	-0.72	1.432	1.593	1.657
Vivianite	-29.372	-19.79	-24.734	-23.528	-26.751
$VO(OH)_2(s)$	-4.829	-2.061	-1.176	0.44	0.968

Table S5. Species sorbed from natural water in presence of 5g/L $MgCO_3$

Component	pH 4	pH 6.8	pH 7.5	pH 10	pH 12	pH 13
/HFA(6)	% sorbed	% sorbed	% sorbed	% sorbed	% sorbed	% sorbed
>SOH(1)	0	0	0	0	0	0
>SOHs2(1)	100	100	100	100	100	100
AsO_4-3	100	100	100	100	100	100
Ca^{+2}	99.97	99.973	99.996	100	100	100
Cd^{+2}	0.012	4.062	3.145	0.217	0.248	0.452
Cl^{-1}	0.038	88.618	97.42	84.457	36.686	1.275
Co^{+2}	0	0	0	0	0	0
CO_3^{-2}	0.005	43.906	79.894	76.358	0.253	0.004
Cu^{+2}	8.916	11.653	7.92	0.428	0	0
F^{-1}	9.799	96.798	94.461	12.03	0.02	0
Fe^{+2}	0	0	0	0	0	0
H^{+1}	0.002	36.773	76.602	99.805	84.371	10.806
H_3AsO_3	11.133	17.199	5.951	216.232	11.831	3.828
Li^{+1}	79.049	97.522	99.24	99.948	96.304	70.187
Mg^{+2}	0	0	0	0	0	0
Mn^{+2}	0	0.527	2.168	3.645	3.462	3.296
$MoO4^{-2}$	0.005	53.66	83.335	67.795	63.155	10.327
Ni^{+2}	99.961	6.678	2.35	17.263	0.382	0.056
$NO3^{-1}$	0.031	79.039	94.884	93.411	0.226	0.001
Pb^{+2}	0	0	0	0	0	0
$PO4^{-3}$	83.241	99.988	99.991	99.451	34.651	0.236
$Sb(OH)_3$	99.981	99.925	99.981	99.997	95.418	28.423
$SeO4^{-2}$	0	0	0	0	0	0
$SO4^{-2}$	21.368	0.078	0.151	0.914	0.01	0
Sr^{+2}	7.652	0.024	0.046	0.363	0.005	0
$Ti(OH)_4$	0.013	4.289	3.258	0.062	0.082	0.183
Tl^{+1}	0	0	0	0	0	0
VO^{+2}	0	0.353	3.442	66.106	80.061	85.625

Table S6. Arsenic species distribution at pH4 and pH 13 in presence of 5g/L $MgCO_3$

pH13				pH4		
Component	% of total concentration	Species name		Component	% of total concentration	Species name
AsO_4^{3-}	5.927	>FehOHAsO_4^{3-} (1)		AsO_4^{3-}	0.029	H_2AsO_4-
	94.072	>FeOHAsO_4^{3-} (1)			1.346	>FehH_2AsO_4(1)
H_3AsO_3	4.965	$HAsO_3^{2-}$			53.874	>FeH_2AsO_4(1)
	24.846	H_2AsO_3-			1.014	>Feh$HAsO_4^-$(1)
	4.16	>Feh$HAsO_3^-$(1)			40.598	>Fe$HAsO_4^-$(1)
	66.027	>Fe$HAsO_3^-$(1)			0.076	>FehAsO_4-2(1)
					3.059	>FeAsO_4^{2-} (1)
				H_3AsO_3	20.95	H_3AsO_3
					0.257	>Fe$HAsO_3^-$(1)
					1.92	>FehH_2AsO_3(1)
					76.866	>FeH_2AsO_3(1)

S5. Arsenic removal from prepared solution

Table S7. Supplementary data for Figure 3.

30 min	0.5g/L		
Initial As C mg/L	qt mg/g	%As removal	Standard deviation initial As concentration
1.0055	1.2674	63.0234	0.0049
3.0125	2.491	41.3444	0.0064
5.266	3.9814	37.8029	0.0594
10.45	7.546	36.1053	0.1273
20.58	10.86	26.3848	0.3536

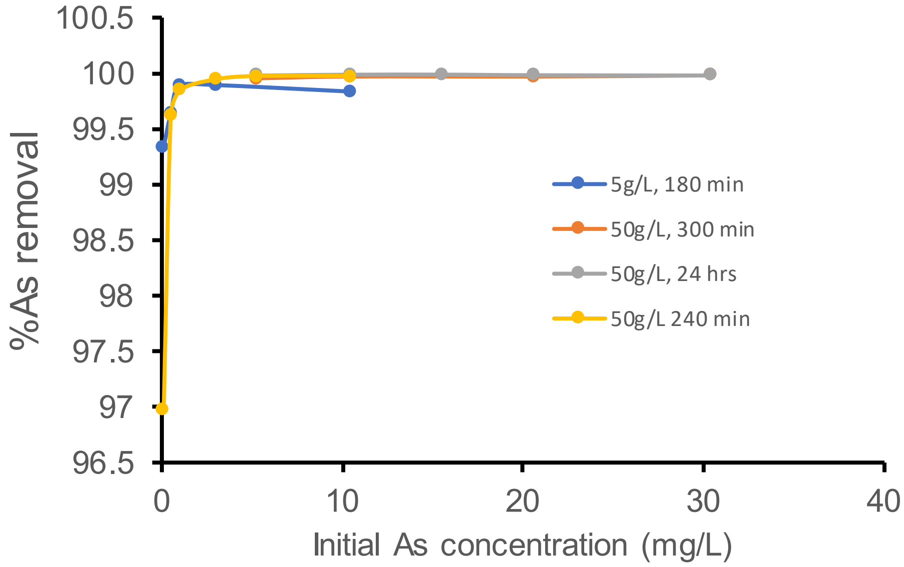

Figure S5. Arsenic removal increases with increase in initial concentration at application of 5g/L magnesite and 50g/L calcined magnesite

Table S8. Data for figure S5 arsenic removal with function of initial concentration

24hr	50 g/L	300 min	50 g/L	240 min	50 g/L	180 min	5 g/L
Initial As	%As	Initial As	%As	Initial As	%As	Initial As	%As removal
5.266	99.98	5.266	99.95	0.1032	96.97	0.1032	99.3
10.45	99.99	10.45	99.97	0.5002	99.63	0.5002	99.6
15.575	99.99	20.58	99.97	1.0055	99.85	1.0055	99.9
20.58	99.98	30.355	99.98	3.0125	99.95	3.0125	99.9
30.355	99.98			5.266	99.98	10.45	99.8
				10.45	99.98		

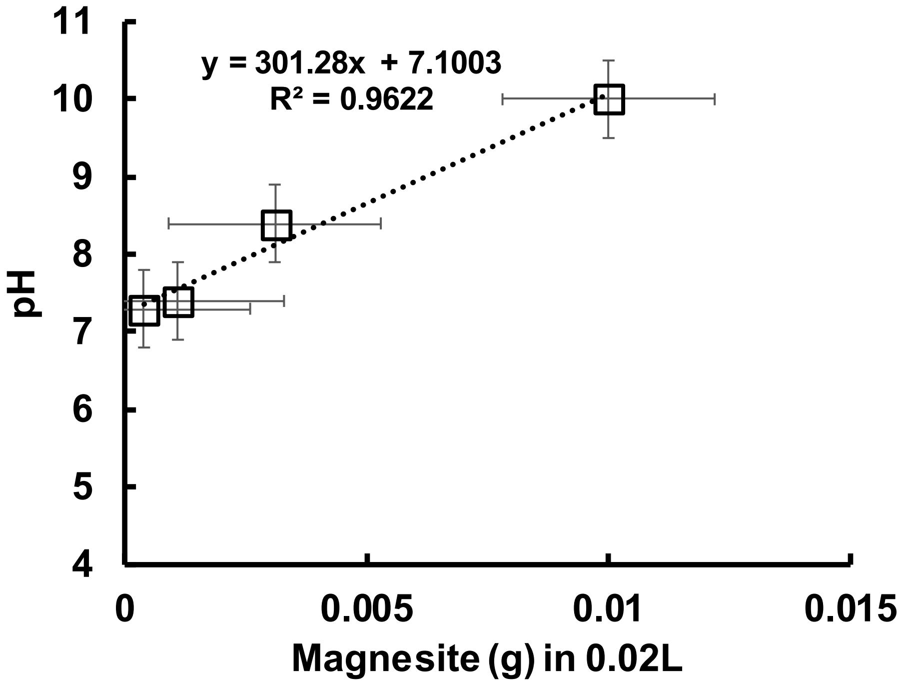

Figure S6. pH increase with function of magnesite dosage

Table S9. Data for Figure 5

Dosage	pH
0.0004	7.3
0.0011	7.4
0.0031	8.4
0.01	10
0.012	10.7
0.014	11.3
0.016	12
0.017	12
0.018	12
0.019	12

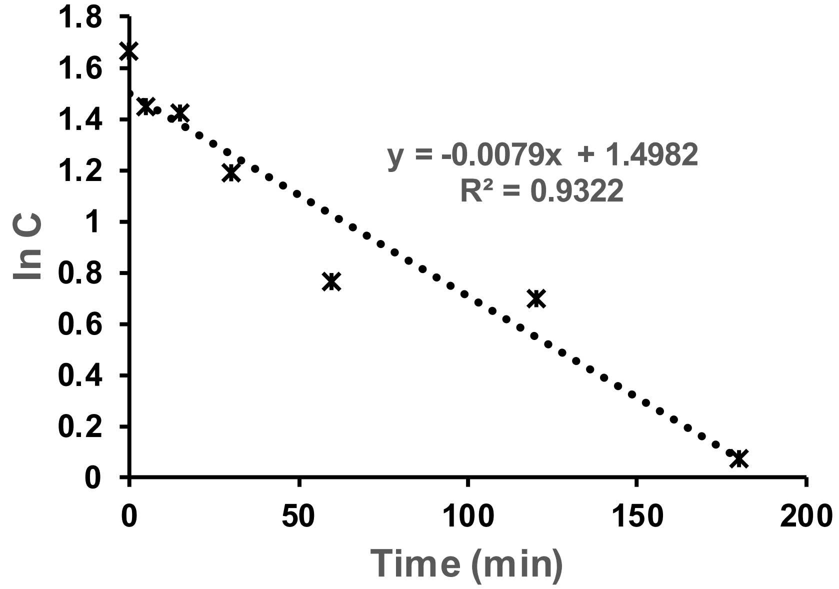

Figure S7. First order rate law

Table S10. Rate laws and half life

5.266 mg/L As	0.5 g/L		5 g/L	50 g/L			0.05 g/L
Time (min)	lnC	Time (min)	lnC	Time (min)	1/C	Time (min)	lnC
0	1.6613	0	1.6613	0	0.1899	0	1.6613
5	1.443	2	0.4874	30	132.8904	5	1.5138
15	1.4205	5	-1.0504	60	169.6929	15	1.4912
30	1.1864	8	-3.3104	120	94.4287	30	1.4985
60	0.7619	15	-3.5059	180	179.019	60	1.5086
120	0.7001	20	-5.1311	240	220.8481	120	1.4992
180	0.0689					180	1.5213
	1st order k =-0.0079, t1/2= 87 min		1st order k =0.3171, t1/2= 2 min		Second order k =0.6324, t1/2= 0.3 min		1st order k = 0.0003, t1/2= 2310 min

Table S11. Pseudo second order, data for Figure 6

Time (min)	Pseudo second order t/qt
5	2.4208
15	6.6566
30	7.5350
60	9.6040
120	18.4502
180	21.4557

Table S12. Freundlich isotherm, data for Figure 7 and Figure 8

0.5 g/L	30min				
Ce	qe	Ce/qe	qe calculated	logce	loqe
0	0	0	0		
0.3718	1.2674	0.2934	5.4484	-0.4297	0.1029
1.767	2.491	0.7094	8.8958	0.2472	0.3964
3.2753	3.9814	0.8227	9.6331	0.50997	0.600
6.677	7.546	0.8848	10.155	0.8246	0.8778
15.15	10.86	1.3950	10.4527	1.1804	1.0358

Table S13. when 0.05g/L calcined magnesite linear regression

Model Summary

Model	R	R Square	Adjusted R Square	Std. Error of the Estimate
1	.957[a]	.915	.873	.53075

a. Predictors: (Constant), pH, Time

ANOVAa

Model		Sum of Squares	df	Mean Square	F	Sig.
1	Regression	12.144	2	6.072	21.556	.007[b]
	Residual	1.127	4	.282		
	Total	13.271	6			

a. Dependent Variable: Conc

b. Predictors: (Constant), pH, Time

Coefficientsa

Model		Unstandardized Coefficients		Standardized Coefficients	t	Sig.
		B	Std. Error	Beta		
1	(Constant)	6.684	1.237		5.406	.006
	Time	-.021	.003	-.959	-6.499	.003
	pH	-.250	.129	-.287	-1.946	.124

a. Dependent Variable: Conc

Table S14. When 0.5g/L calcined magnesite is applied

Model Summary

Model	R	R Square	Adjusted R Square	Std. Error of the Estimate
1	.975[a]	.950	.926	.07933

a. Predictors: (Constant), pH, Time

ANOVA[a]

Model		Sum of Squares	df	Mean Square	F	Sig.
1	Regression	.482	2	.241	38.309	.002[b]
	Residual	.025	4	.006		
	Total	.507	6			

a. Dependent Variable: Conc
b. Predictors: (Constant), pH, Time
Coefficientsa

Model		Unstandardized Coefficients B	Unstandardized Coefficients Std. Error	Standardized Coefficients Beta	t	Sig.
1	(Constant)	6.913	.270		25.580	<.001
	Time	.001	.001	.212	1.663	.172
	pH	-.245	.029	-1.060	-8.319	.001

a. Dependent Variable: Conc

Table S15. When 5g/L in 2, 5, 8, 15, 20 minutes is applied for As removal

Model Summary

Model	R	R Square	Adjusted R Square	Std. Error of the Estimate
1	.973[a]	.946	.910	.62431

a. Predictors: (Constant), pH, Time

ANOVA[a]

Model		Sum of Squares	df	Mean Square	F	Sig.
1	Regression	20.415	2	10.208	26.189	.013[b]
	Residual	1.169	3	.390		
	Total	21.585	5			

a. Dependent Variable: Concentration
b. Predictors: (Constant), pH, Time

Coefficients[a]

Model		Unstandardized Coefficients B	Unstandardized Coefficients Std. Error	Standardized Coefficients Beta	t	Sig.
1	(Constant)	11.747	1.792		6.556	.007
	Time	-.166	.036	-.621	-4.605	.019
	pH	-.965	.187	-.695	-5.150	.014

a. Dependent Variable: Concentration

Table S16. When 50g/L calcined magnesite is applied to remove arsenic

Model Summary

Model	R	R Square	Adjusted R Square	Std. Error of the Estimate
1	.997[a]	.995	.992	.19729

a. Predictors: (Constant), pH, Time

ANOVA[a]

Model		Sum of Squares	df	Mean Square	F	Sig.
1	Regression	22.949	2	11.475	294.799	<.001[b]
	Residual	.117	3	.039		
	Total	23.066	5			

a. Dependent Variable: Conc

b. Predictors: (Constant), pH, Time

Coefficients[a]

Model		Unstandardized Coefficients		Standardized Coefficients	t	Sig.
		B	Std. Error	Beta		
1	(Constant)	13.019	.550		23.658	<.001
	Time	-.003	.001	-.116	-2.484	.089
	pH	-1.143	.057	-.938	-20.144	<.001

a. Dependent Variable: Conc

S6. Artificial intelligence neural network

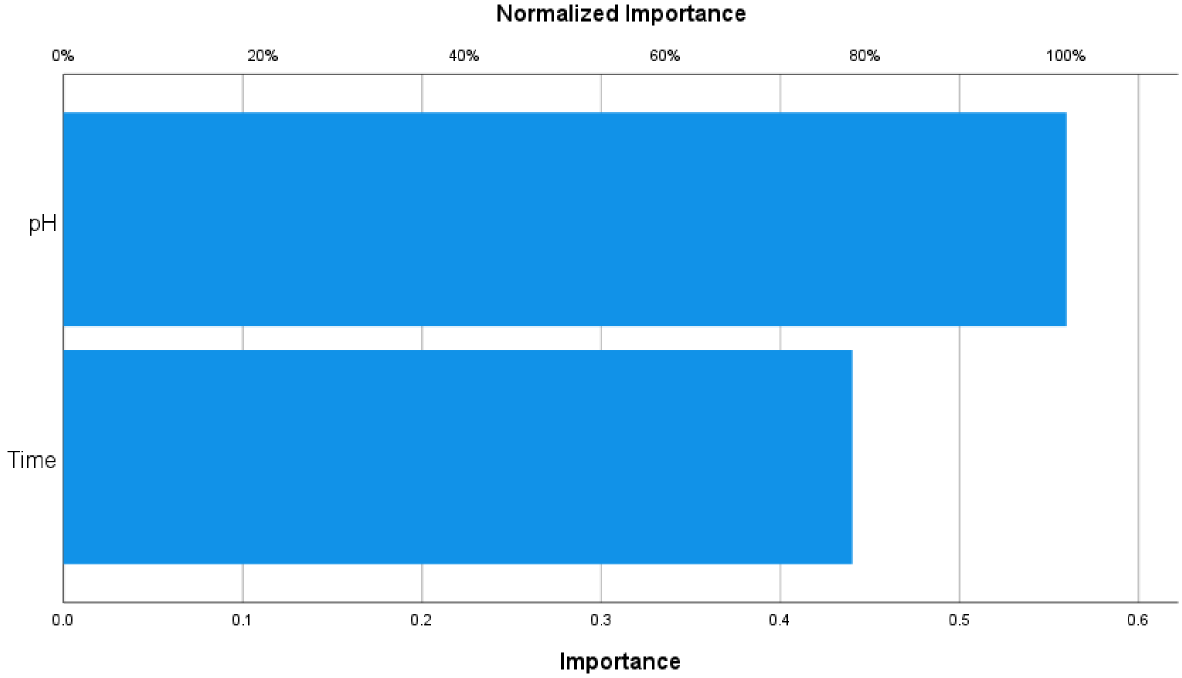

Figure S8. Artificial intelligence neural network shows pH influence removal process.

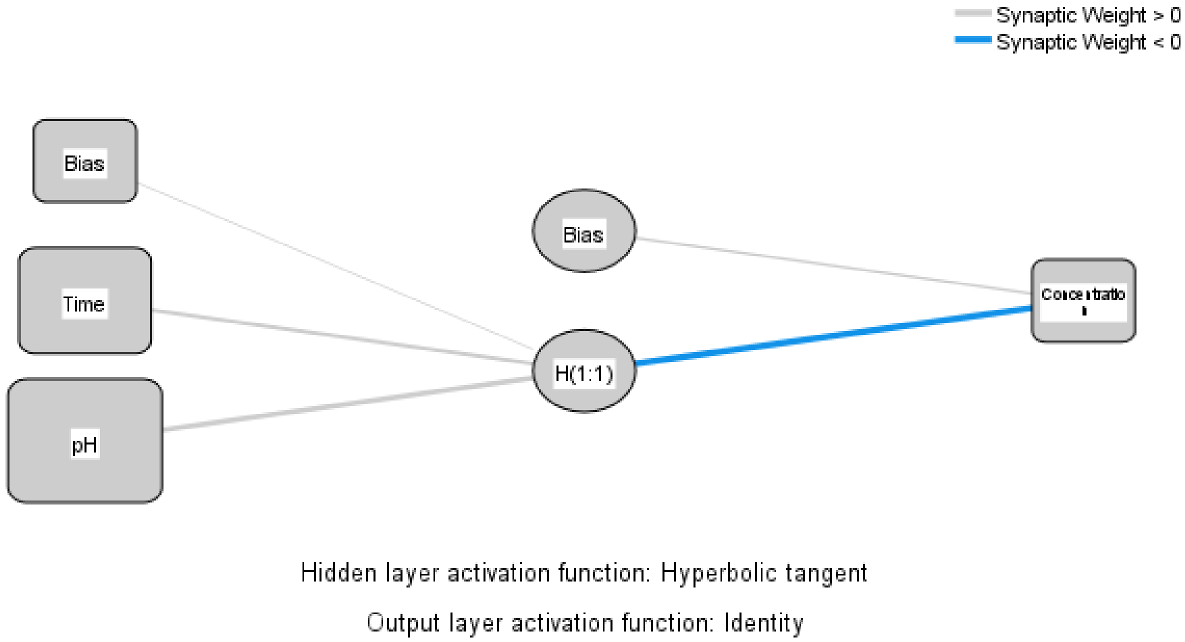

Figure S9. Artificial intelligence shows strong correlation to pH

Table S17. Artificial Neural Network

Independent Variable Importance

	Importance	Normalized Importance
Time	.440	78.7%
pH	.560	100.0%

Parameter Estimates

Predictor		Predicted: Hidden Layer 1 H(1:1)	Predicted: Output Layer Concentration
Input Layer	(Bias)	.387	
	Time	.856	
	pH	.882	
Hidden Layer 1	(Bias)		.428
	H(1:1)		-1.374

Model Summary

Training	Sum of Squares Error	.026
	Relative Error	.013
	Stopping Rule Used	1 consecutive step(s) with no decrease in error[a]
	Training Time	0:00:00.00
Testing	Sum of Squares Error	.069
	Relative Error	.[b]

Dependent Variable: Concentration

a. Error computations are based on the testing sample.

b. Cannot be computed. The dependent variable may be constant in the testing sample.

The rate constant for intraparticle diffusion (Kid) is given By Weber Morris (Bulut et al 2007)

$$q_t = K_{id}t^{1/2} + C \qquad \text{Equation S1}$$

Where C is the intercept. Best fit straight that do not pass through the origin indicating that there are an initial boundary layer resistance.

The simple linear regression model is

$$y = mx + c + \mathcal{E} \qquad \text{Equation S2}$$

From the Freundlich straight line equation, the kf can help to calculate the free energy change ΔG° of the sorption for both anions using equation S3

$$\Delta G^o = -RT\ In(k_f \times 1000) \qquad \text{Equation S3}$$

Where R is the gas constant (0.00831447 kJ/Kmol) and Tis the temperature in Kelvin. The negative free energy indicates the feasibility of the process and the spontaneous of the adsorption (Chiban et al 2011)

The hydrolysis reactions underline the process of water alkalization upon contact with magnesium containing minerals. Dissociation reactions are responsible for the saturation of water with magnesium ions (Shadrunova et al 2022).

$MgCO_3 + H_2O \leftrightarrow (MgOH) + HCO_3^-$ equation S4 stage 1

$(MgOH)+ +H_2O \leftrightarrow Mg(OH)_2$ equation S5 stage 2

S7. Chemical reactions rates and isotherms

The removal reaction batch experiment was fitted on pseudo second order (Equation S6) to investigate how fast the rate of reaction occurs between magnesite and As. However, half-life was calculated from first order reaction rate law (Equation S7) to determine how long As is halved to its original value.

$$\frac{t}{q_t} = \frac{1}{k_2 q_e^2} + \frac{t}{q_e} \qquad (Equation\ S6)$$

$$t_{1/2} = \frac{In2}{k} \qquad (\ Equation\ S7)$$

The relationship between the amount of As removed and the concentration of As remaining in solution is described by reaction isotherms (Masindi and Gitari, 2016). The most used reaction isotherm model for liquid/solid phase is the Freundlich (Equation S8, S9) isotherm. This model describes removal reaction process on heterogenous (multilayer) surface (Masindi and Gitari, 2016).

To achieve isotherm, the 0.5 g/L, 5 g/L, 50 g/L calcined magnesite was introduced in 1, 3, 5, 10, 20 mg/L As solution and shaked for 30 minutes. The Freundlich reaction isotherm describes the heterogenous surface energy by multilayer adsorption.

$$q_e = K_f C_e^{\frac{1}{n}} \qquad \text{(Equation S8)}$$

The equation S8 may be linearized by taking the logarithm of both sides of equation to form Equation S9.

$$log q_e = \frac{1}{n} log C_e + log K_f \qquad \text{(Equation S9)}$$

where C_e is equilibrium concentration (mg/L), q_e is amount removed at equilibrium (mg/g), K_f is partition coefficient (mg/g) and "n" is intensity of removal.

The linear plot of log q_e versus log C_e indicates if the data is described by Freundlich reaction isotherm.

The value of K_f implies that the energy of contaminant removal on a homogeneous surface is independent of surface coverage and "n" is an adsorption constant which reveals the rate at which removal is taking place. These two constants are determined from the slope and intercept of the plot of each other.

The D-R isotherm model is of important to understand the type of removal mechanism by plotting the graph of $lnCe$ angainst $\mathcal{E}^2$ (equation S10, 11, 12) and calculate the sorption energy Es which is correlated with "k" (isotherm constant) (Bakatula et al., 2017).

$$lnC_e = lnq_m - k\mathcal{E}^2 \qquad \text{(Equation S10)}$$

Where q_m is the maximum sorption capacity of sorbent (mg/g), $\mathcal{E}$ is the Polanyi potential, R is the gas law constant 8.3145 kJ/mol K, T is the absolute temperature K,

$$\mathcal{E} = RT\, ln\left[\left(1 + \frac{1}{C_e}\right)\right] \qquad (Equation\ S11)$$

$$E_s = \frac{1}{\sqrt{-2 \times k}} \qquad (Equation\ S12)$$

)

If the *Es* is less than 8 kJ/mol, the process of adsorption is physisorption (ion-ion attraction). When *Es* is between 8 and 16 kJ/mol, the process of adsorption is ion-exchange, but for *Es* greater than 16 kJ/mol, the process of adsorption is chemisorption involving the formation of covalent bonds (Bakatula et al., 2017).

The As removed by magnesite at any time (t) was determined from the Equation S13 (Wang et al., 2018)

$$q_t = \frac{(C_0 - C_t)V}{m} \qquad (Equation\ S13)$$